Arc-parallel strain in a short rollback-subduction system: The structural evolution of the Crotone basin (northeastern Calabria, southern Italy)

Margaret A. Reitz[1] and Leonardo Seeber[2]

Received 28 September 2011; revised 22 June 2012; accepted 25 June 2012; published 11 August 2012.

[1] Calabria, located in southern Italy, is the exposed part of the forearc in the Ionian/Tyrrhenian subduction-rollback boundary. We present a tectonic model for the evolution of Calabria during the last 12 Ma that incorporates the structure and stratigraphy of the Crotone basin. At the re-initiation of rollback, we document listric normal faults that accommodated a deep-rooted extensional regime. Extension ceased in the Tortonian and did not continue throughout rollback. The middle Tortonian to early Messinian is characterized by distal sedimentation despite rapid rollback. Westward verging thrusts in Tortonian sediments and olistrostrome deposits within the Messinian section can be explained by instabilities in the accretionary wedge during the Messinian salinity crisis. Tectonic quiescence returned to the basin after the crisis and continued until a north-south shortening event in the middle Pliocene. Our kinematic data and new evidence of two basin inversions suggest arc-parallel shortening of the forearc. We propose that this shortening correlates with the passage of the forearc through the Apulia-Nubia narrow. This data also dispute previous interpretations of the Crotone basin as a pull-apart or transtensional basin. The identification of the main structures in the Crotone basin suggest a shift from quiescence to upheaval, beginning with Pliocene arc-parallel shortening associated with the passage of the forearc through the Apulia-Nubia narrow and continuing until today.

Citation: Reitz, M. A., and L. Seeber (2012), Arc-parallel strain in a short rollback-subduction system: The structural evolution of the Crotone basin (northeastern Calabria, southern Italy), *Tectonics*, *31*, TC4017, doi:10.1029/2011TC003031.

1. Introduction

[2] The Calabrian Arc was first interpreted as a subduction-rollback system by *Malinverno and Ryan* [1986], dispelling previous models that relied on vertical motion of the crust. Large-scale tomographic and geodynamic studies [e.g., *Bonardi et al.*, 2001; *Faccenna et al.*, 2001, 2004; *Barberi et al.*, 2004; *Rosenbaum and Lister*, 2004] have shown that rollback of this system has displaced Calabria at least 1200 km over the last 35 Myr. This subduction-rollback occurred in two phases: the early phase opened the Liguro-Provençal Basin between 35 Ma and 16 Ma and the second, or Calabrian phase, opened the Tyrrhenian Sea (12 Ma–present) [*Patacca et al.*; 1990; *Gueguen et al.*, 1998; *Faccenna et al.*, 2001; *Rosenbaum et al.*, 2002; *Nicolosi et al.*, 2006].

[3] The Calabrian subduction system is akin to the Aegean Arc and Betic-Rif Arc, which are small, "Mediterranean-type" subduction zones characterized by episodic rollback, a complex downgoing plate geometry, and a thick accreting oceanic sedimentary sequence [*Faccenna et al.*, 2004]. It has been suggested that episodic rollback is related to changes in the rate of African plate motion [*Jolivet and Faccenna*, 2000; *McClusky and Relinger*, 2010]. Interactions and collision with buoyant continental lithosphere control the length of these arcs and may also affect their rollback velocity and internal structure. Such changing constraints on the subduction regime are generally absent from oceanic subduction systems, even those with dimensions similar to the Mediterranean arcs, such as the Banda and South Scotia Arcs. Changes in rollback velocity and/or lateral constraints will induce changes in backarc, forearc, and accretionary wedge tectonics, but what these effects are and in which part of the subduction system they will be felt is poorly understood [e.g., *Patacca et al.*, 1990; *Jolivet and Faccenna*, 2000; *Nicolosi et al.*, 2006; *D'Agostino et al.*, 2008, 2011].

[4] As the Calabrian Arc was translated to the southeast, the northern and southern edges of the forearc interacted with the irregular continental boundaries of NW-SE trending Apulia and E-W trending Nubia. Block rotations along the African coast [e.g., *Guarnieri*, 2004] and Apulia [e.g.,

[1]Department of Earth and Environmental Science and Lamont-Doherty Earth Observatory, Columbia University, Palisades, New York, USA.
[2]Lamont-Doherty Earth Observatory, Palisades, New York, USA.

Corresponding author: M. A. Reitz, Department of Earth and Environmental Science and Lamont-Doherty Earth Observatory, Columbia University, Palisades, NY 10964, USA. (reitz@ldeo.columbia.edu)

0278-7407/12/2011TC003031

Muttoni, *et al.*, 2000] are examples of deformation structures typical of the forearc during oblique collision. Strike-slip faulting along the boundaries has also been observed along the Sangineto line and Mt. Kumeta-Alcantara line (Figure 1a) [*Ghisetti and Vezzani*, 1981]. In this manuscript, we document changes in the deformation of the northern part of the forearc basin as it approaches and eventually collides with Apulia. By documenting how and when deformation occurs over the last 12 Myr, we are able to reevaluate the structures that respond to frontal changes in accretion tectonics versus other structures that take up strain during the oblique collision. In particular, we are able to establish a "base-line" of forearc deformation to which the current Pleistocene deformation can be compared.

2. The Crotone Basin

[5] The Crotone basin, located in northeastern Calabria, east of the Sila Massif (Figure 1) is an ideal place to investigate structures associated with episodic rollback and complex boundaries. It contains a sedimentary record from the Calabrian phase of subduction-rollback. Although the stratigraphy of the Crotone basin is well documented [*Ogniben*, 1955, 1962; *Roda*, 1964, 1967; *Roveri et al.*, 1992; *Moretti*, 1993; *Zecchin et al.*, 2003, 2004a, 2006; *Mellere et al.*, 2005; *Capraro et al.*, 2006; *Barone et al.*, 2008], the tectonic evolution of the forearc basin remains uncertain. The Crotone basin is partially subaerial, but the basin continues offshore to the south and east, merging with what is generally considered an active forearc basin [*Minelli and Faccenna*, 2010]. The Sila Massif and San Nicola Fault (SNF) bound the basin to the west and north, respectively (Figure 1). The transition to arc massif acting as the backstop to accretion complex occurs just offshore northern Calabria [*Roveri et al.*, 1992; *Minelli and Faccenna*, 2010]. Therefore, according to the *Dickinson and Seely* [1979] classification, the Crotone basin is a constructed basin (at least since 12 Ma), where the sediments were deposited unconformably across a structural discontinuity between the arc massif (inner basin) and deformed accreted strata (outer basin). This boundary, the static backstop [*Kopp and Kukowski*, 2003], may be inactive during a steady state subduction regime, but is likely activated during profound reorganizations of the accretion system. This setting is typical for a forearc basin and ideal for distinguishing between shallow-rooted, local structures and deep-rooted, regional structures that deform the static backstop (Figure 2).

[6] The stratigraphy of the Crotone basin is divided into three sedimentary cycles, separated by regional unconformities (Figure 3) [*Roda*, 1964]. The first cycle (Serravallian to early Messinian) contains four lithologic units: the San Nicola Formation, a basal conglomerate and sandstone; the Tortonian Ponda Formation, a marine sandstone deepening to clay and marl that conformably overlies the San Nicola Formation; the early Messinian Tripoli Formation, a thin, diatomaceous layer; the Messinian Lower Evaporite Formation. The transgressive deposits of the San Nicola and Ponda formations are interpreted to correlate with re-initiation of subduction-rollback, ~12 Ma, and basin formation. During the early Messinian (7 Myr–6 Myr), marls of the Ponda Formation are interbedded with sapropels and diatomites (Tripoli Fm), signifying the onset of the salinity crisis [*Krijgsman et al.*, 1999]. The Lower Evaporite Formation is composed of limestone and gypsum [*Roda*, 1964] and represents the gradual brining of the Mediterranean Sea, although the connection to the Atlantic Ocean probably remained open throughout deposition [*Flecker and Ellam*, 2006; *Ryan*, 2009]. This part of the section is largely absent from our field area. An angular unconformity caps this cycle and is generally attributed to "mid-Messinian tectonics" [*Roda*, 1964]. Most recently, this unconformity has been interpreted as a consequence of the isostatic readjustment of the accretionary wedge following desiccation of the Mediterranean [*Cavazza and DeCelles*, 1998].

[7] The second tectono-stratigraphic cycle, from the middle Messinian through and including the early Pliocene, has four main units: the Detrital Salt Formation, Upper Evaporite Formation, the Cavalieri Clay, and the Zinga Formation [*Roda*, 1964]. The evaporite deposits in our work area are largely composed of detrital gypsum and halite and we lump them under the title "Messinian units." The Carvane Conglomerate, a fluvial conglomerate, caps the evaporite sequence. The provenance of the Carvane Conglomerate is unique: derived from accretionary material to the east, different from all other sediments in the Crotone basin, which are sourced from basement rocks to the west [*Barone et al.*, 2008]. The Cavalieri Clay marks the end of the salinity crisis and return to deep-water conditions. The Zinga Formation is comprised of three unconformity-bounded sequences [*Zecchin et al.*, 2003]. *Zecchin et al.* [2004a] determined that deposition in each sequence was controlled by listric normal faults and the unconformities were caused by NE-trending growth folds, tentatively ascribed to salt diapirism. A widespread angular unconformity caps this stratigraphic cycle and is related to a tectonic event in the basin [*Roda*, 1964; *Van Dijk*, 1992].

[8] One unit, described in detail by *Ogniben* [1955], does not fit into Roda's three sedimentary cycles: the argille varicolori or accretionary material. This unit crops out at different stratigraphic levels throughout the study area and consists of varicolored clays, distal sandstones and shales, and fragments of deepwater limestones and igneous rocks. *Ogniben* [1955] interpreted tongues of this unit as orogenic nappes emplaced from east to west in addition to having characteristics of an olistrostrome (gravitational collapse). It was, according to *Ogniben* [1955], emplaced in multiple events, during, but also before the Messinian; it is not interbedded with post-Messinian units. Accretionary material with similar stratigraphic positions crop out along the northern coast of Calabria [*Cavazza and Barone*, 2010]. In southern Calabria, similar units were also identified, but attributed to an earlier event in the middle Miocene [*Amodio Morelli et al.*, 1976; *Cavazza and DeCelles*, 1998; *Cavazza and Ingersoll*, 2005; *Cavazza and Barone*, 2010].

[9] The final cycle (middle Pliocene and Pleistocene) is largely made up of outer-shelf to slope mudstones of the Cutro Clay. The Cutro Clay is underlain by a transgressive sequence of lagoonal to shallow marine deposits (Spartizzo Clay and Scandale Sandstone) and is capped by the regressive Strongoli Sandstone. The Strongoli Sandstone is the last deposit before the Crotone basin was uplifted above sea level [*Roda*, 1964; *Mellere et al.*, 2005; *Zecchin et al.*, 2006]. Lack of sedimentation, however, did not necessarily mark the end

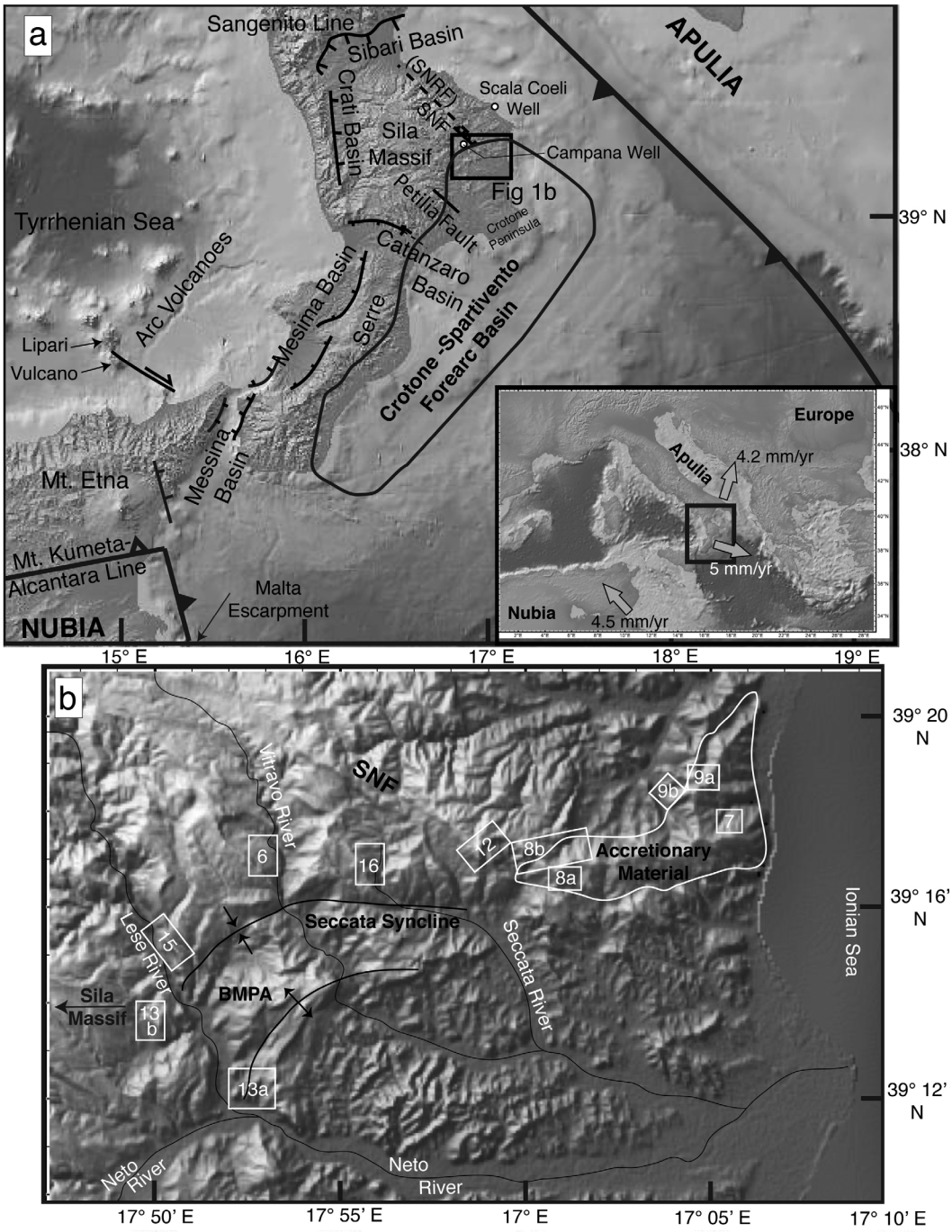

Figure 1. (a) The main tectonic features around Calabria, including the Pleistocene arc-parallel basins (Crati and Mesima) and arc-perpendicular basins (Sibari, Catanzaro, Messina). The Sila Massif is the square-shaped, topographic high in northern Calabria. The forearc basin, as defined by *Minelli and Faccenna* [2010] is outlined in black. Also shown are the two strike-slip faults (SNRF and Petilia) hypothesized by *Van Dijk* [1992] to control deposition and deformation in the Crotone basin; this work investigates only the southeastern part of the SNRF, here called the SNF. The box is the outline of the study area. Inset: shows regional topography as well as GPS velocities from *D'Agostino et al.* [2008]. Nubia and Adria velocities are shown in an European reference frame, while Calabria is shown with a Nubia reference frame. (b) A GeoMapApp image of the study area highlights the morphology and main tectonic features: Linear topographic features to the north mark the SNF, the BMPA is highlighted in the south by an anticline-syncline pair (arrows). White boxes show the locations of figures throughout the manuscript.

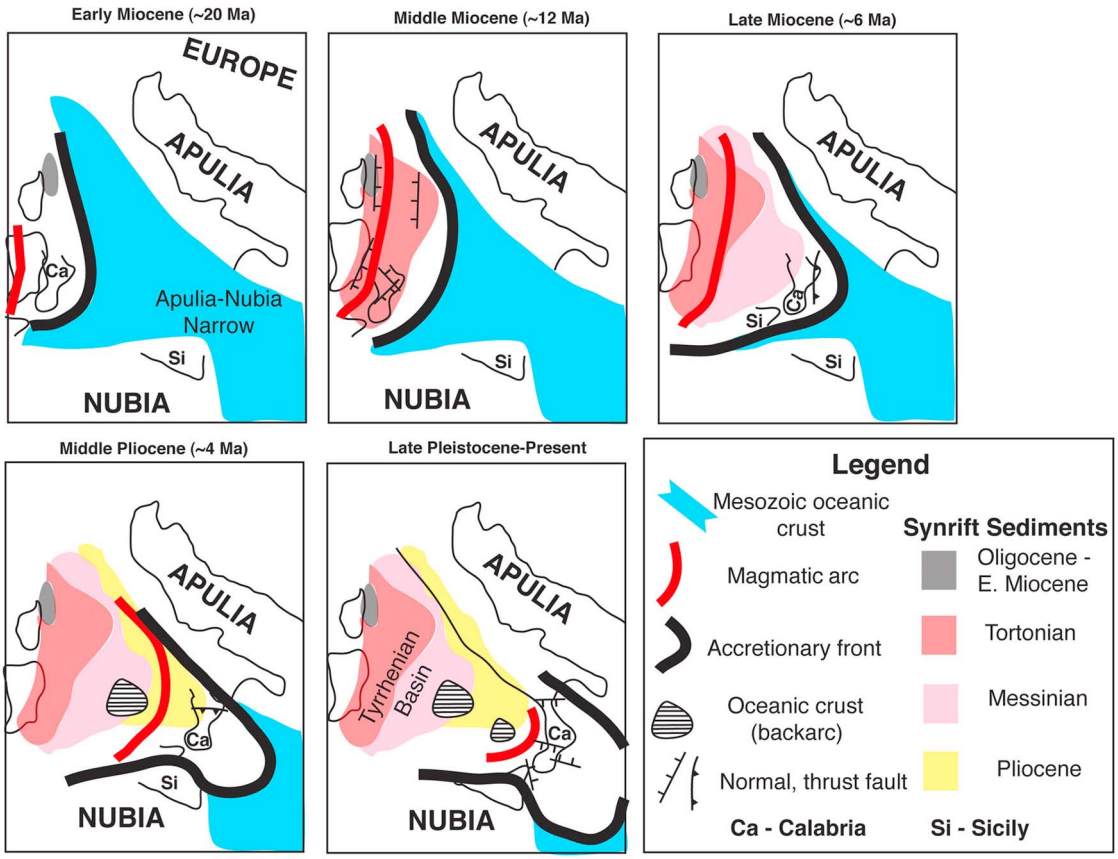

Figure 2. Evolution of Tyrrhenian basin during the Calabrian phase of subduction-rollback, adapted from *Gvirtzman and Nur* [2001]. Constraints on the synrift sediments, magmatic arc, and oceanic crust are compiled from *Rosenbaum and Lister* [2004]. The tectonic features and location of Calabria, itself, are changed slightly according to our interpretation of data presented in this manuscript. Coupling between the backarc and forearc may have been easier at the re-initiation of rollback, when the distance between the two was at a minimum; the "syn-rift" sediments are not confined to the backarc, sedimentation occurred throughout the forearc and backarc during rollback, but the deformation and style of sedimentation are likely different in these two distinct tectonic settings.

of the Crotone basin as a fundamental structural feature in the active Calabrian forearc.

3. Methods

[10] We collected structural data from sedimentary rocks in the northern part of the Crotone basin (Figures 1 and 4). Mapping and structural analysis of inverted basins, growth structures, and meso-scale stress and strain indicators were combined to distinguish and characterize distinct phases in the tectonic evolution of the Crotone basin. We then interpreted these events in the context of published regional data and, more generally, the evolution of the Calabrian phase of subduction. Our new structural data were collected during five field campaigns from 2007 to 2011 and are synthesized in a map and five cross sections, shown in Figures 4 and 12, as well as lower hemisphere, equal area stereonet plots in Figures 5, 7, 10, and 14. Published geologic maps and stratigraphy by the Italian Geological Survey (1958–1962), *Roda* [1964], and *Zecchin et al.* [2003] provided the base maps for Figure 4a. In the titles of the sections below, the ages given are meant to be of structures occurring during that time period.

4. Serravallian–Tortonian Structures: Quiescence After Initial Extension and Subsidence

4.1. Observations

[11] In the Crotone basin, the San Nicola and Ponda formations, together, record Serravallian to early Messinian times, 12–6 Myr. Generally, the San Nicola Formation is thin, a few tens of meters. We document several syn-depositional normal faults locally thickening the San Nicola Formation. These faults have various orientations, but are generally striking east-west to northwest-southeast (Figure 5). Where exposed, these faults are rooted in the basement and extend upsection, locally thickening the Ponda Formation. Figure 6 shows 120 m of Ponda Formation exposed in the hanging wall and 80 m of un-faulted and fine-grained Ponda Fm above the fault. Messinian units crop out extensively in the study area, but the deep-rooted normal faults are never seen to displace or thicken them. The San Nicola Formation crops

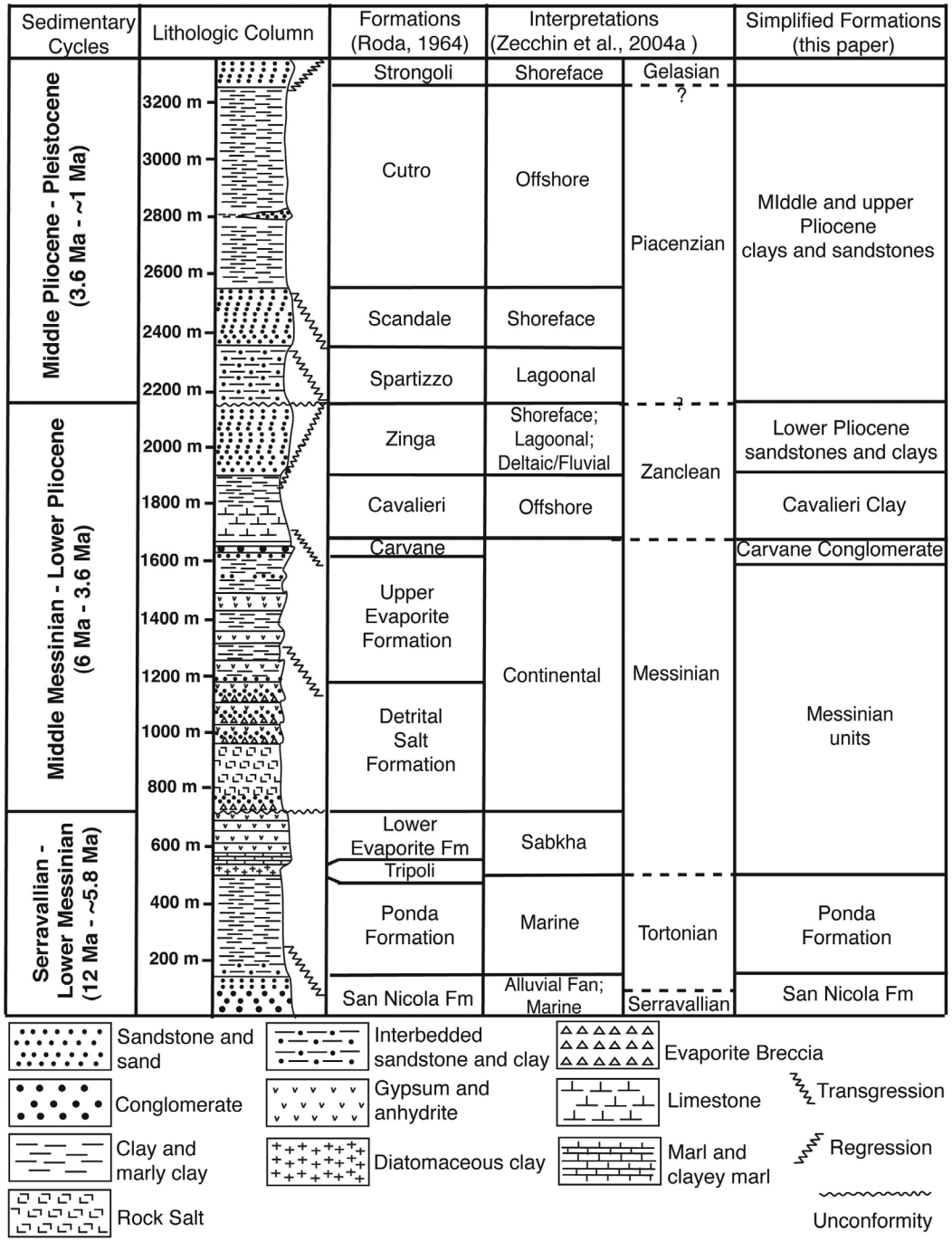

Figure 3. Summary of the stratigraphy in the Crotone basin, focusing on pre-Pleistocene times and on units that pertain to our structural data. Sedimentary cycles discussed in section 3 are shown on left with names and interpretations of units that guided us in our interpretations [*Roda*, 1964; *Zecchin et al.*, 2004a]. The last column contains the terminology used in this manuscript and its relation to the literature.

out more extensively to the north and west, therefore, our sampling of these syn-depositional normal faults is likely to be incomplete.

[12] The San Nicola Fault (SNF), located in the northern part of the study area, is the largest of the syn-sedimentary normal faults. Our data and discussion pertain only to the southeastern end of the San Nicola-Rossano Fault (SNRF, mapped by *Van Dijk* [1992]), therefore we use the name SNF rather than SNRF to clarify the locations of our observations. The SNF is a multistranded fault zone that strikes NW-SE and dips to the northeast. It is expressed by a topographic high cored by hundreds of meters of the conglomeritic facies of the San Nicola Formation. The SNF juxtaposes San Nicola Formation to the north with younger Ponda Formation to the south. The San Nicola Formation varies in thickness from 30 m on the south side of the fault (Campana 1 Well,

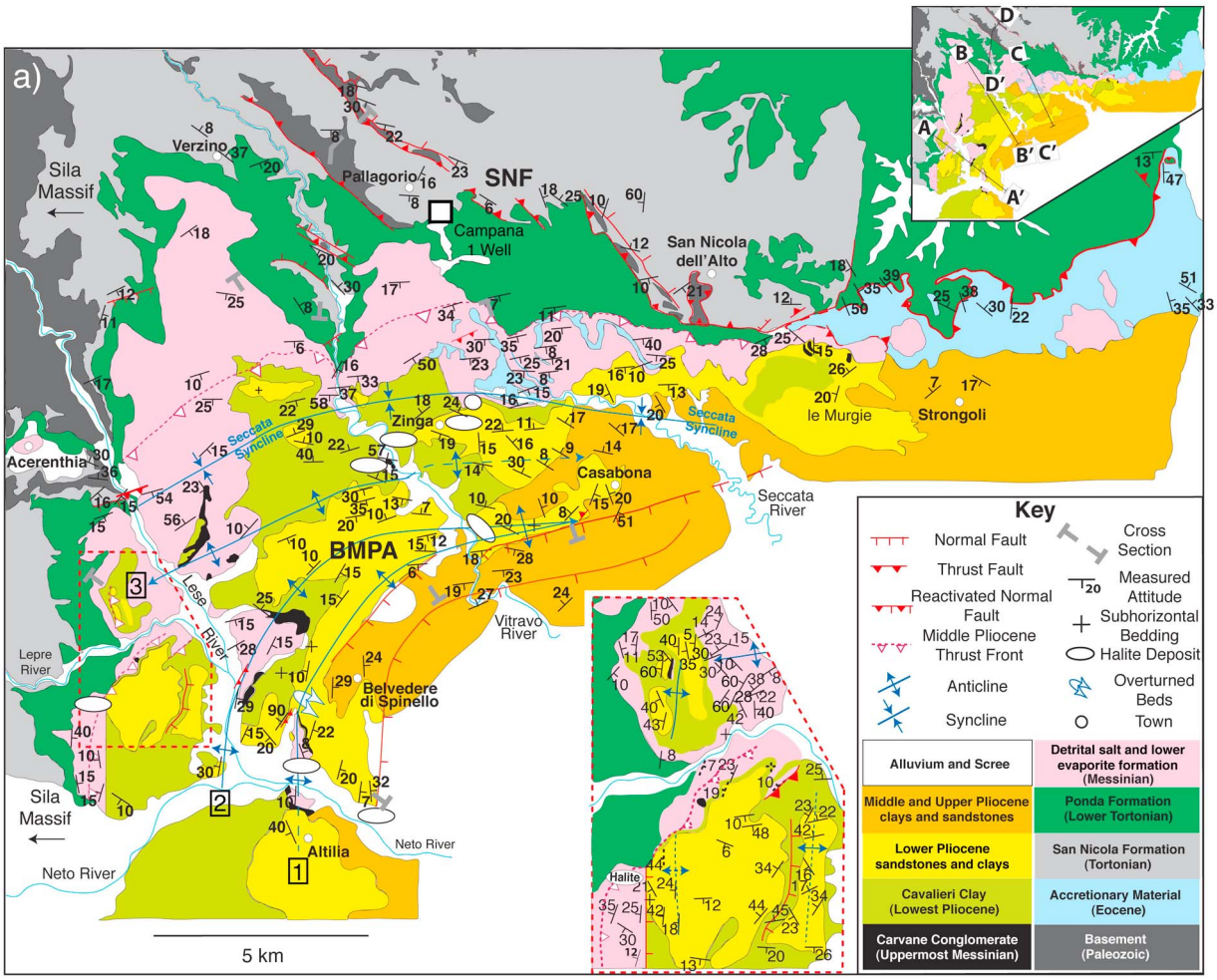

Figure 4. (a) Data compiled from our field campaigns (2007–2011); base geology map after *Zecchin et al.* [2003]. BMPA contains three anticlines (1, 2, 3 labeled) that converge to the east; SNF bounds the Crotone basin in the northwest. The red dotted inset shows details in the area west of the Lese River. The locations of the cross sections are on the inset map at the top. The unit descriptions are in Figure 3. The color key is the same as in the cross sections. (b) Cross sections show the main structures in the study area at 1 × 1 scale. All sections are constrained by bedding attitudes near the sections, which are projected on the cross sections at the appropriate elevations. D = halite diaper. For section A, the BMPA is interpreted as a fault-bend fold rooted in a ramp marking the SE flank of the BMPA. This fault is reactivated as a normal fault in the Pleistocene (see text). The flat above this ramp continues until the Lese River, where it ramps upsection. Smaller thrust faults branch off this main thrust generating anticlines in the Pliocene and Messinian sediments. Circled regions show outcrops with an older over younger relationship (inset in Figure 4a). Section B is based on exposures along the Lese and Vitravo rivers. It highlights the Seccata Syncline, the ramp through the Messinian section, and a normal growth fault through the Serravallian-Tortonian sequence (at 3500 m and Figure 5). The normal fault coincides with the base of the ramp and may have nucleated it. The imbrication is inspired by the outcrop in Figure 16. In section C, blind faults in this section are inferred from anticlines. Sections A and B are based on outcrop evidence. These faults become blind, but the related folding can be traced to the east. Also, folds 1, 2, and 3 merge into a single anticline along the SE flank of the BMPA that, with the Seccata Syncline, dominate the morphology. Section D crosses the SNF and shows its multiple branches. Most faults were originally normal growth faults, evidenced by the thickened San Nicola Formation in their hanging walls. Some of them have been reactivated as thrust faults forming mesoscale hanging wall anticlines or inverted basins, which are marked in the section.

Figures 1a and 4a) to more than 400 m on the north side. The thickness of this formation decreases to 300–350 m at the Scala Coeli Well (Figure 1a), which is 20 km from the fault zone.

4.2. Interpretation of Serravallian-Tortonian Structures

[13] The multidirectional normal faults and fining-upward trend recorded in the San Nicola and Ponda formations

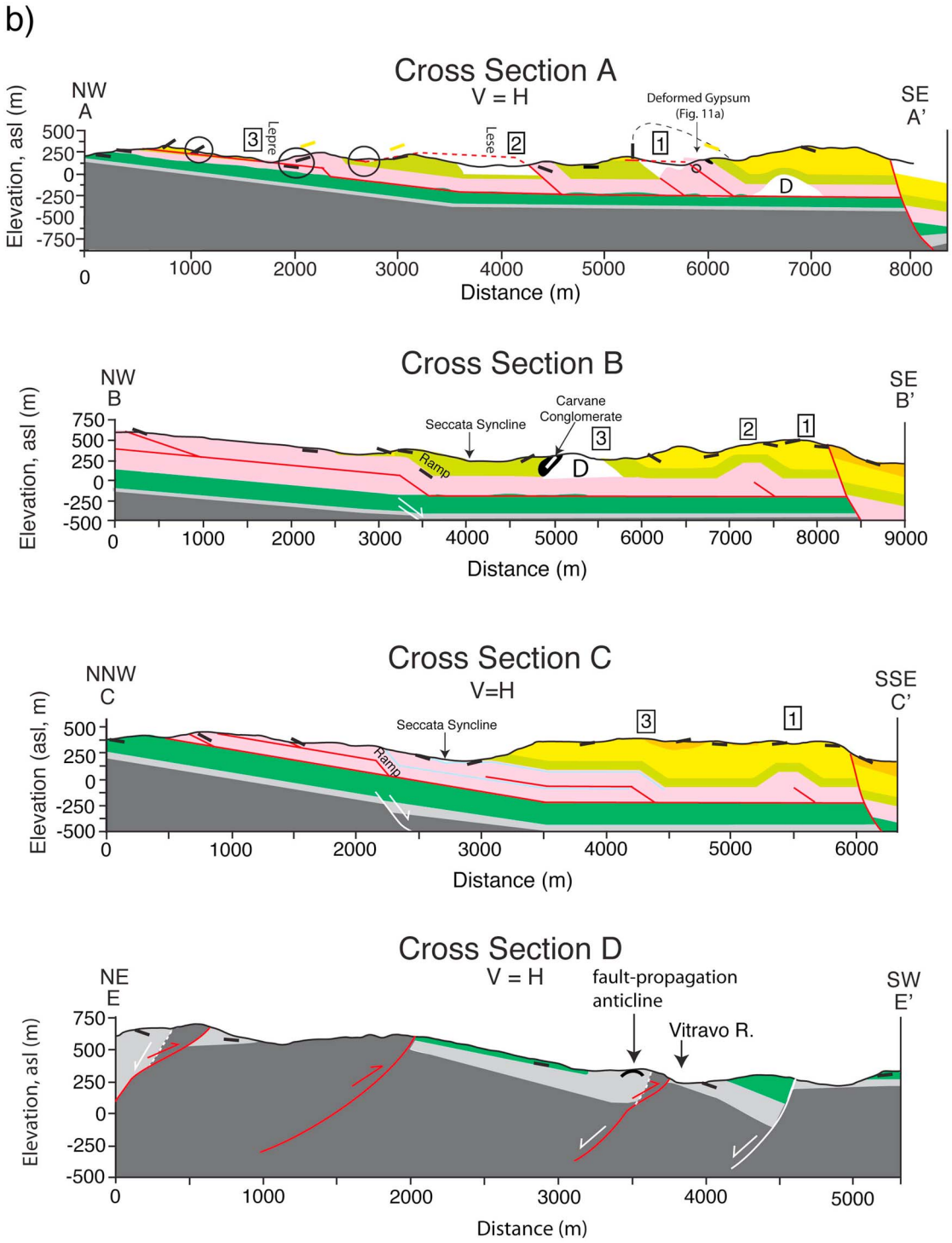

Figure 4. (continued)

imply extension and subsidence in the Crotone basin. This extensional phase is widespread across Calabria [*Vai and Martini*, 2001; *Mattei et al.*, 2002; *Cavazza and Ingersoll*, 2005]. In the Crotone basin, these normal faults are rooted in basement and terminate upsection in the Ponda Formation. Assuming a relatively constant sedimentation rate for the Ponda Formation, we interpret the fault terminations to suggest an end to forearc extension in the early to middle Tortonian. Extension and drowning of the forearc were, therefore, synchronous with the rifting that separated Calabria from Sardinia, suggesting a region of upper-plate extension that affected the backarc as well as the entire

forearc at the re-initiation of rollback. Extension in the forearc did not continue during steady subduction-rollback as evidenced by the fault terminations in the Ponda Formation. Although we expect southeastward-directed shortening structures generated by accretion, the San Nicola and Ponda formations contained only extensional structures. This suggests that at least the internal part of the Calabrian forearc basin was shielded from accretion tectonics, possibly by the underlying continental fragment and/or the fossil accretion structure inherited from the Lower Miocene subduction-rollback phase [*Kopp and Kukowski*, 2003].

[14] The SNF was the largest structure active in the study area during the re-initiation of rollback. Thickness changes and fanning of the beds of both the San Nicola and Ponda formations toward the SNF are features consistent with sediments deposited in a half graben, bounded by a NE-dipping listric normal fault. None of these faults, including the SNF, display direct evidence of large transcurrent motion coupled with extension, although a component of transcurrent motion cannot be ruled out. Taken together, however, the distribution and geometry of these faults (Figures 4 and 5) is inconsistent with a pull-apart or block-rotation model in a transtensional system dominated by sinistral motion [e.g., *Christie-Blick and Biddle*, 1985], as suggested in the literature [*Van Dijk*, 1992]. We, therefore, propose instead that the Serravallian-Tortonian phase in the Crotone basin was dominated by deeply rooted extension accommodated by syn-sedimentary, listric normal faults.

[15] During the remainder of the first tectono-stratigraphic cycle, tectonics were remarkably peaceful in the Crotone basin. The thick, fine-grained, and sub-horizontal Ponda Formation recorded a long period of tectonic quiescence despite very rapid arc rollback. This interpretation is supported by *Krijgsman et al.* [1999], who correlated the layering in the Ponda Formation to the 11 kyr precession cycle and documented a gradual brining of the sediments in the early Messinian. The small, climate-related variations in chemistry they resolve would likely be overprinted by larger changes in sedimentation typical in areas with active, local tectonics. The extraordinary peacefulness indicates that, during the mid-Tortonian to early Messinian, the forearc basin was unaffected by either shortening in the accretionary wedge or extension in the Tyrrhenian Sea. This requires localizing extension in the backarc shortly after the re-initiation of rollback and maintaining a dynamic equilibrium during rapid, but steady rollback.

5. The Messinian Salinity Crisis: Changes in Accretion Dynamics

5.1. Observations

[16] Structures in the Carvane Conglomerate and the accretionary material from which it is derived yield new insights into the effects of the Messinian salinity crisis on the accretion process. The large exposure of accretionary material in the northeast of the study area (Figures 1b and 4a) displays coherent structure from the mesoscale to the kilometer scale with only rare chaotic structures. A clear structural trend of clay, shale, mudstones, and chert beds display isoclinal folds where well exposed (Figure 7). In some places, the hinges of the folds have been eroded away, leaving only the stacked fold limbs behind. These measurements are compiled into the stereonet in Figure 7. The pervasive, coherent structure manifests strong west-southwest vergence and large amounts of shortening.

[17] A ridge top quarry exposes a fault contact between the Messinian units and the accretionary material (Figure 8a). This fault strikes 120°, consistent with the shortening direction obtained from the isoclinal folds, but with opposite vergence. The accretionary material at this outcrop wedges under a gypsum bed and folds it up, separating it from the gypsum bed below. Thrusting involves not only Messinian units, but reaches into the underlying Ponda Formation. In Figure 9a, Ponda Formation is highly deformed and in contact with the accretionary material in one thrust sheet. However, it is well bedded and coherent in a higher thrust sheet. A southwesterly transport direction is more evident in Figure 9b: where Ponda Formation is thrusted over Ponda Formation without deforming the clay beds in the hanging wall. The spatial relationship between the two thrust contacts is sketched in Figure 9c.

[18] From east to west, the accretionary material becomes thinner and more chaotic, losing its systematic structure. In the central part of the study area, the accretionary material appears as thin mélange layers wholly within Messinian units (Figure 4a, northeast of Casabona). This mélange displays the chaotic structure typical of an olistostrome. Accretionary material does not appear deeper in the stratigraphy, as we see to the east. Therefore, we identify a transition between regionally coherent thrust emplacement and isoclinal folding in the east to chaotic olistrostrome deposits in the central part of the study area.

[19] In addition to the structure in the accretionary material, we mapped several outcrops of the Carvane Conglomerate, the uppermost unit of the Messinian. We recognized two characteristics of the unit that are ubiquitous in the study area. First, there is a systematic fracturing of the cobbles (Figure 10, insets). These fractures do not propagate into the matrix. En echelon fractures are seen in some of the clasts, but, in general, the fractures appear to be extensional joints recording the direction of the minimum stress, σ_3. The maximum compressive stress, σ_1, is in the plane of the fractures [*Eidelman and Reches*, 1992]. The attitudes of the fractures are generally consistent within and among outcrops (Figure 10). This fracture pattern is remarkably pervasive and consistent, but does not propagate up or down section and is prominently absent from the San Nicola Formation, a Serravallian, conglomeritic facies similar to the Carvane Conglomerate. The second unique feature is that the cobbles in the conglomerate are well-rounded and typically 5–20 cm in diameter, as expected in a fluvial deposit. However, the matrix is composed of angular, coarse sand. The matrix material also fills many of the cracks in the clasts (Figure 10, insets).

5.2. Interpretation of Messinian Structures

[20] We identified a transition in the accretionary material from a tectonic emplacement in the external part of the forearc basin to a sedimentary olistostrome in the internal part. This observation constrains the timing of this event and suggests a possible mechanism of emplacement. The sedimentary olistostromes are restricted to Messinian units. The base of the accretionary unit in the Crotone basin rests directly on top of the Ponda Formation and has been interpreted as a pre-Messinian emplacement [*Ogniben*, 1955;

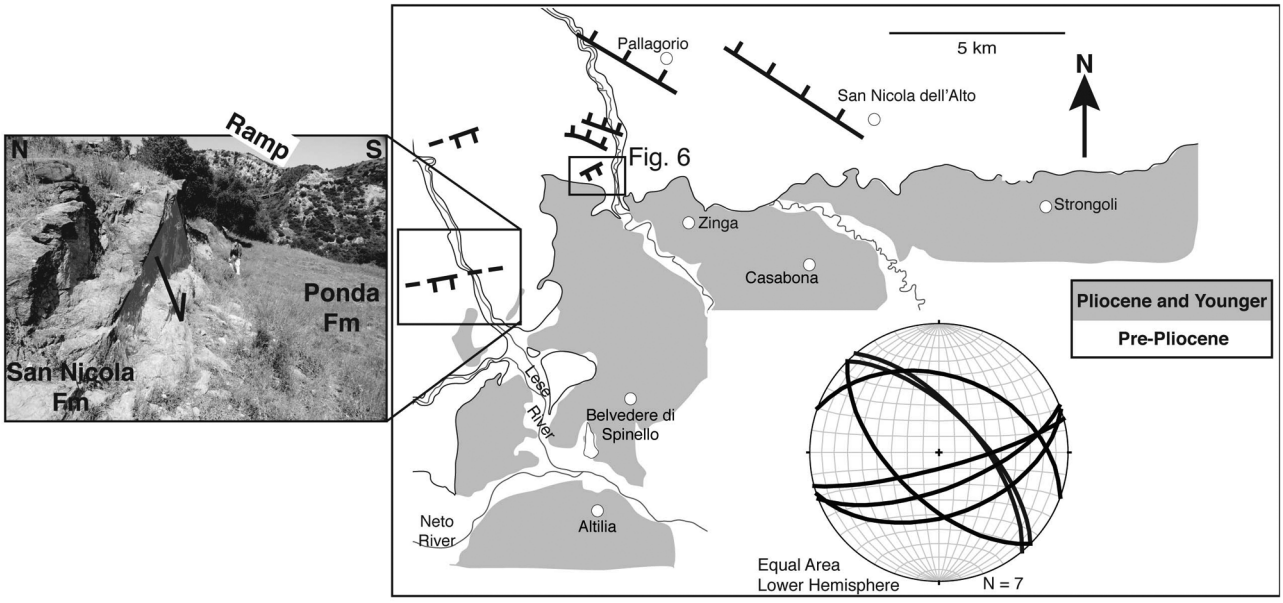

Figure 5. Simplified map of the field area, highlighting the Serravallian-Tortonian normal faults. They are rooted in the crystalline basement and are syndepositional with the San Nicola Formation. The faults are multidirectional and do not define a clear direction of extension. Inset: Photo of western-most fault showing fault activation in the Tortonian and the spatial correlation of this fault with the Pliocene contractional ramp in the background.

Cavazza and Barone, 2010]. However, this contact is tectonic and is included in a thrust stack that reaches deeper into the Ponda Formation (Figure 9b), the emplacement must be younger than the hanging wall sediments: Ponda Formation and Messinian units. We do not see evidence for an east-west shortening in post-Messinian units, thereby restricting this shortening event to the Messinian, coincident with olistostrome deposition and the Messinian salinity crisis. *DeCelles and Cavazza* [1995] and *Cavazza and DeCelles* [1998] link the deposition of Messinian conglomerates in southeastern Calabria to changes in taper of the accretionary wedge caused by the Messinian salinity crisis. We pursue this idea to account for the accretionary material emplacements. Evaporation of 4 km of water from the accretionary wedge [*Ryan*, 2009] likely generated a subcritical wedge [*Davis*, *et al.*, 1983]. In order to restore criticality, backthrusting in the rear of the accretionary wedge is expected. This backthrusting reached the external part of

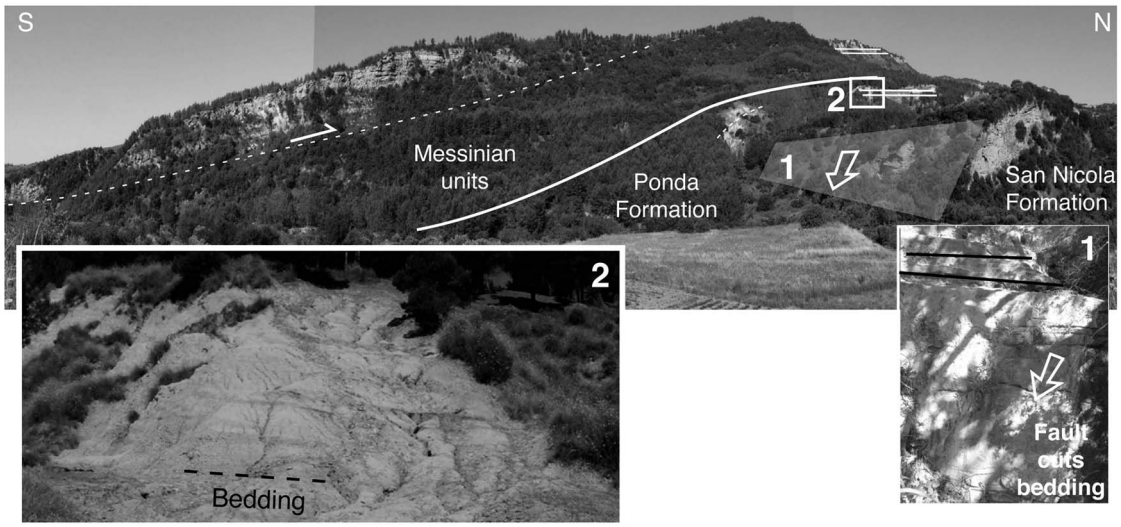

Figure 6. Serravallian-Tortonian normal fault (inset 1). Despite thickness changes across the fault, flat-lying Ponda Formation and Messinain units above the fault (inset 2) show this extensional faulting ended in the early to middle Tortonian.

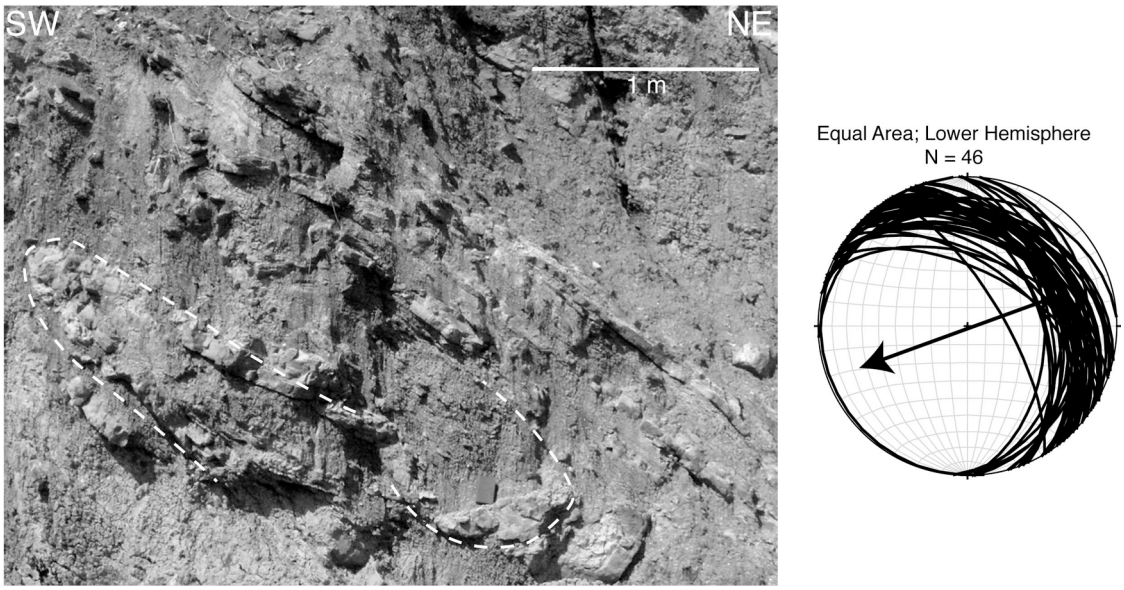

Figure 7. Example of isoclinal folds in the accretionary material emplaced onto the Crotone basin. The hinges of many of the folds have been obliterated by the extreme strain, but the limbs are clear. 46 limb attitudes on equal area, lower hemisphere stereonet projections are from seven widely distributed outcrops. The consistent stacking orientation of these beds manifest a strong west-southwestward shortening and vergence.

the forearc basin (eastern part of the study area) generating the west-verging thrust structures, opposite from the direction associated with accretion, in the Ponda Formation and Messinian units. Thrusting in the east of the Crotone basin is, therefore, constrained to occur after the early Messinian.

[21] The olistostrome deposits in the central part of the study area are found solely within Messinian units and suggest a sedimentary origin. We hypothesize that backthrusting during the beginning of the salinity crisis created a structural high to the east of the forearc basin. Once this high was significant, slope failures generated olistostromes that flowed to the west. These flows would have been discrete events during the "normal" detrital gypsum sedimentation, signifying an offshore high.

[22] Eventually, the entire forearc basin became subaerial, evidenced by the deposition of the Carvane Conglomerate. Gravity flows continued to occur during this deposition. Interestingly, the direction of shortening from the Carvane fractures is similar to the direction of shortening determined from the folds in the accretionary material, suggesting a genetic relationship. Since the fractures do not continue in the underlying or overlying sediments, we conclude that a pervasive stress event occurred for a short time and at shallow depths, when the Carvane Conglomerate was at or near the Earth's surface. Since, most of the fractures are steep (Figure 10), we can rule out a causative horizontal decompression. We can also rule out an increase in vertical stress (caused by the re-flooding of the Mediterranean), which predicts steep fractures with variable strikes. Therefore, the most plausible cause of the fractures is a pulse of horizontal compression parallel to the fractures. The angularity of the matrix suggests that this sandy component of the unit was deposited without much fluvial reworking. The injection of the matrix into the fractures (Figure 10) suggests the juvenile matrix arrived at or during the fracturing. Although other hypotheses are possible, we propose that these fractures were generated during the flooding of the Mediterranean at the end of the salinity crisis. Flooding created a supercritical wedge, which collapsed to restore criticality. High-velocity submarine flows flowed down the river valleys created during the subaerial stage and fractured previously deposited clasts of the Carvane and injected angular matrix into the deposit. Downslope transient stresses require fracture orientations that reflect the westward drainage pattern from the offshore high, as we see. Our interpretation is summarized in Figure 11. There are two other stress events that may have generated these fractures: First, a Pliocene shortening event (discussed below) generates a stress oblique to the fracture direction and can be ruled out. Second, a Pliocene extensional phase [*Zecchin et al.*, 2003] generated a stress regime subparallel to the fractures, but is restricted to Pliocene and Pleistocene sediments.

[23] Late Messinian conglomerates in southeastern Calabria have been studied by *DeCelles and Cavazza* [1995] and *Cavazza and DeCelles* [1998]. Paleocurrent directions and lithologies in these conglomerates show a proximal source to the west, co-located with the current Serre Massif. *Massari et al.* [2010] document southward paleoflow in the Carvane Conglomerate just south of our study area and argue for a "Sila" source. This is in contrast with our study area, where lithologies, paleoflow directions, and backthrusting argue for a source east of the forearc. In an evaporated Mediterranean Sea, there is likely to be a high collocated with Sila and Serre Massifs and is still consistent with our model. The combined evidence show that backthrusting during the salinity crisis had a major effect along the entire Calabrian forearc, but these effects varied and merit further investigation of offshore sediments.

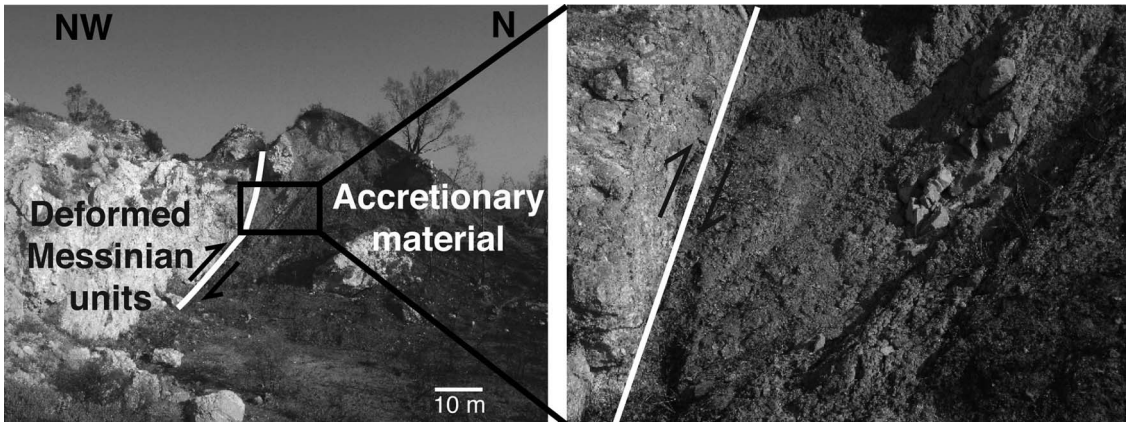

Figure 8. Contact between accretionary material and Messinian units. Accretionary material is thrusted under the lighter Messinian unit, which is folded upward.

[24] *Cavazza and Barone* [2010] have proposed strike slip motion along the SNF and/or incipient collision of the accretionary wedge with Apulia as possible mechanisms for accretionary emplacement in the Messinian. We are skeptical on both counts. The thrust sheets involve Ponda Formation and younger cover, but not the basement or San Nicola Formation, in which the SNF is rooted. Furthermore, we find no evidence of large strike-slip motion on the SNF. Collision of the northern edge of the accretionary wedge with Apulia accompanied the southeastward rollback of Calabria, shortened the forearc, and brought the Crotone basin progressively closer to this boundary. Direct effects of the collision in the basin would be expected to increase after the Messinian. In contrast, the emplacement of the accretionary material into our study area abruptly ends at the Miocene-Pliocene boundary. Our data show that the backthrusting is limited to the salinity crisis and possibly just to the latest phase of the crisis. This coincidence is suggestive of a causal relation considering that the crisis is more than an order of magnitude shorter than the 12 Myr duration of Calabrian subduction and accretion and because major readjustment of the wedge is expected as a result of the crisis.

6. Pliocene Arc-Parallel Contraction

[25] Two, structural and topographic highs dominate the morphology of the study area: the San Nicola Fault (SNF) and the Belvedere-Montagna Piana Anticlinorium (BMPA) (Figures 1b, 4a). Both these structures probably accommodated arc-parallel contraction during the Pliocene.

6.1. San Nicola Contractional Structure: Observations and Interpretation

[26] The SNF was described in a previous section as a listric, normal fault bounding a half graben to the north and active in the Serravallian-early Tortonian. The current morphology and structure, however, suggest a different, more recent deformation event. The hanging wall sediments are 200–400 m above the footwall sediments. At the southeastern edge of the SNF, the thick hanging wall sediments are folded into an anticline (Figure 12a). This anticline is difficult to trace along strike due to erosion. Similar anticlines are evident in the hanging walls of the other Serravallian-Tortonian normal faults (Figure 4b, section D). Along the forward limb of this anticline, basement outcrops are juxtaposed with conglomerates of the San Nicola Formation. Both the basement slivers, which can be up to a kilometer in length, and the conglomerates are highly brecciated, suggesting significant strain. Nevertheless, they are ridge-forming, erosion-resistant units relative to the incompetent cover rocks of the Ponda Formation.

[27] The reverse offset between hanging wall and footwall sediments, the anticlinal hanging wall, and the presence of basement slivers along the forward limb of the anticline all point to a listric normal fault reactivated in contraction. We interpret the basement slivers to be indicative of footwall shortcut geometry. The upper reach of the SNF is steep (Figure 5), however, the dip of the fault decreases with depth. When subjected to a shallow-dipping maximum stress, these faults reactivated as thrusts at depth, but were unfavorably oriented so that new faults broke forward into the footwall and effectively transferred slivers of the footwall (basement in this case) into the hanging wall (Figure 12b). Overall, the amount of shortening taken up in this reactivation is minor. The spectacular topographic relief of the SNF was formed by a modest, but deep-rooted, contractional event and differential erosional resistance.

[28] Timing of basin inversion and contraction of the SNF is broadly constrained to post-Messinian and pre-Pleistocene. Messinian units abut the SNF on the south side and are well bedded and tilted away from the SNF. No thickness or facies changes are detected in the Messinian units or Carvane Conglomerate toward the fault zone, as would be expected in syntectonic sediment approaching an active structural high. Furthermore, we have argued for a gravitational event in the late Messinian that requires a topographic low co-located with the SNF throughout the Messinian. Therefore, basin inversion must postdate the Messinian. On the other hand, such inversion is unlikely to occur in the Pleistocene, when deformation in the Crotone basin and in the rest of Calabria is largely extensional. These observations restrict the shortening event to the Pliocene, where evidence for a deep-rooted contraction already exists [*Van Dijk*, 1992; *Massari et al.*, 2010] (and below). Therefore,

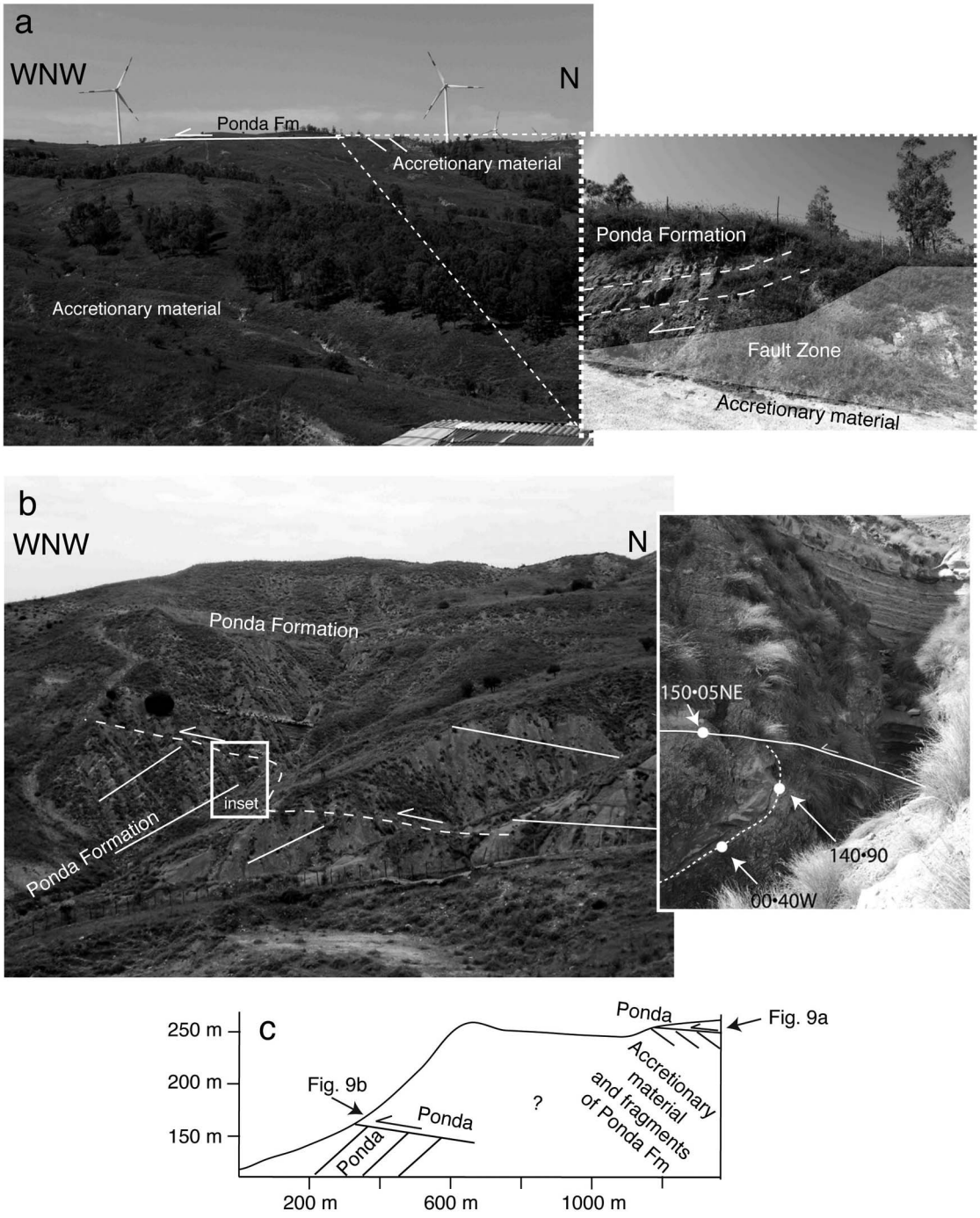

Figure 9. Westward emplacement onto the Crone basin of accretionary material and Ponda formation by stacked thrust sheets. (a) Ponda Formation over accretionary material in a thurst, not a sedimentary or olistrostromic contact, which allows for a Messinian age of emplacement. (b) WSW verging thrust fault within the Ponda Formation consistent with the vergence from the isoclinal folding of accretionary material, Figure 7. (c) Section subparallel to transport direction showing the relative positions of Figures 9a and 9b.

we propose that shortening along the SNF is coeval with the middle Pliocene event as the least-astonishment hypothesis.

6.2. The Belvedere–Montagna Piana Anticlinorium: Observations

[29] The Belvedere–Montagna Piana Anticlinorium (BMPA) is a topographic high that rises 100 to 300 m above the surrounding land, located south of the SNF. In map view, it curves in a broad arc concave to the southeast and is cut by several river valleys (Figures 1b and 4a). Erosion-resistant Zinga Formation forms the topographic high.

[30] In the western part of the study area, the core of the BMPA is exposed. Figure 13a shows an eroded, asymmetric anticline verging to the northwest and breached by the thrust

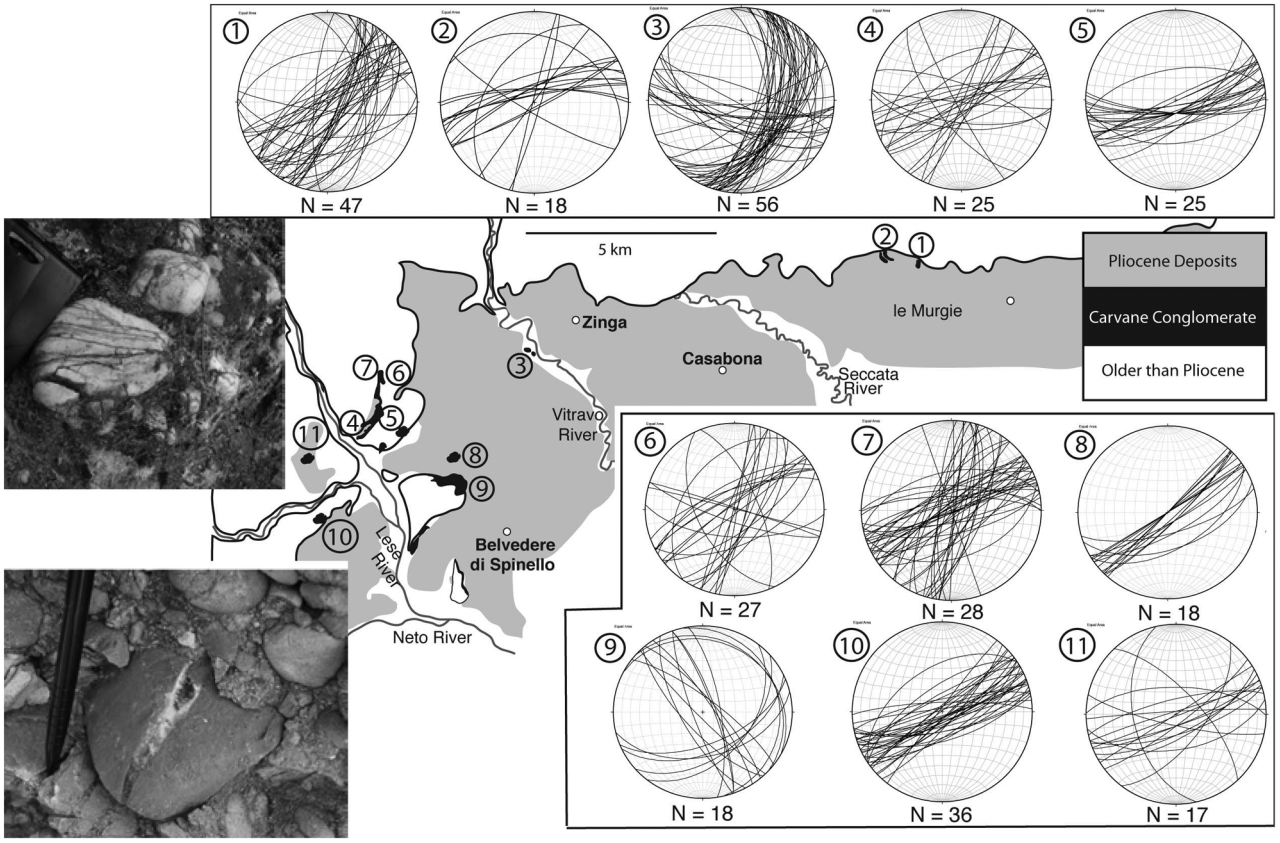

Figure 10. Systematic fractures in Carvane Conglomerate pebbles. Insets are photos of extensional joints and matrix injection typical of the clasts in the Carvane Conglomerate. Simplified field map shows the locations of the 11 outcrops from which we collected fracture orientations, which data are plotted on equal area, lower hemisphere stereonet projection. The strike of the extensional joints, NW-SE, is similar to the direction of emplacement of the accretionary material, suggesting a causal relation.

fault at its core. Inset 1 shows sub-vertical Zinga Formation in the forelimb atop sub-horizontal Cavalieri Clay. This incompetent clay marks the thrust contact. Zinga Formation on the backlimb, east of the anticline core, is flat lying to moderately dipping. The fault controlling this fold is coincident with the subhorizontal Cavalieri Clay. In order to account for the geometry of southeast limb of the anticline, the exposed fault is likely to be the flat updip of a ramp in the subsurface (Figure 4b, section A). This fold can be traced via bedding and mesoscale contractional structures to the northeast and east as fold #1 of the BMPA (Figure 4).

[31] A second fault-controlled fold (#2 in Figure 4) crops out on both sides of the Lese River. The fault is within the Messinian units and deformation associated with this fault extends into Pliocene sediments (Figure 4b, section A). The fold can be traced via bedding for a short distance before it merges with fold #1 in the east. This fault is steep, suggesting it is an imbricate from the basal thrust. The third and outermost fold of the BMPA is located north of the Lepre River (Figure 13b, fold #3 in Figure 4). It is at the same stratigraphic level as fold #1: steeply dipping Zinga Formation overlies a subhorizontal thrust fault, coincident with the Cavalieri Clay. All three of these folds require a flat-lying thrust fault in the subsurface that roots them (Figure 4b, section A). Between folds #2 and #3, we find examples of the older over younger relationship expected in a thrust system (Figure 4b, section A). The exposure is poor because they exist in weak clay layers. The ramps off the basal thrust rarely offset the Cavalieri Clay; instead, they become flats within the Cavalieri Clay masking this relationship.

[32] Continuing updip, thrust faults are exposed deeper in the stratigraphy. In the Messinian units, the dominant shortening structures are faults. Their attitudes and transport directions are consistent with the folds of the BMPA (Figure 14). The most spectacular structure of this Pliocene thrust system is a flat-ramp-flat that doubles the Messinian section. This structure is best exposed along the Lese River and can be traced for 18 km to the east guided by its clear expression in the bedding-controlled morphology (Figures 4 and 15). The ramp is exposed again at the Vitravo River, though the transition from ramp to flat is less clear. The Seccata River, further east, exposes the tip of a fault that carried a horse from the ramp onto the top flat (Figure 16). Another thrust sheet covers this horse, suggesting an imbricate system. The strike of this structure is 70° in the west and bends to E-W (84°–94°) in the east. This arcuate shape mirrors the changing strike of the Pliocene bedding that delineate the BMPA to the south. The flat-ramp-flat structure in the Messinian sediments (Figure 15) and the asymmetric folds of the BMPA indicate a similar vergence, to the north and northwest. A regional syncline, here named the Seccata Syncline (Figures 1b and 4) is expressed by a

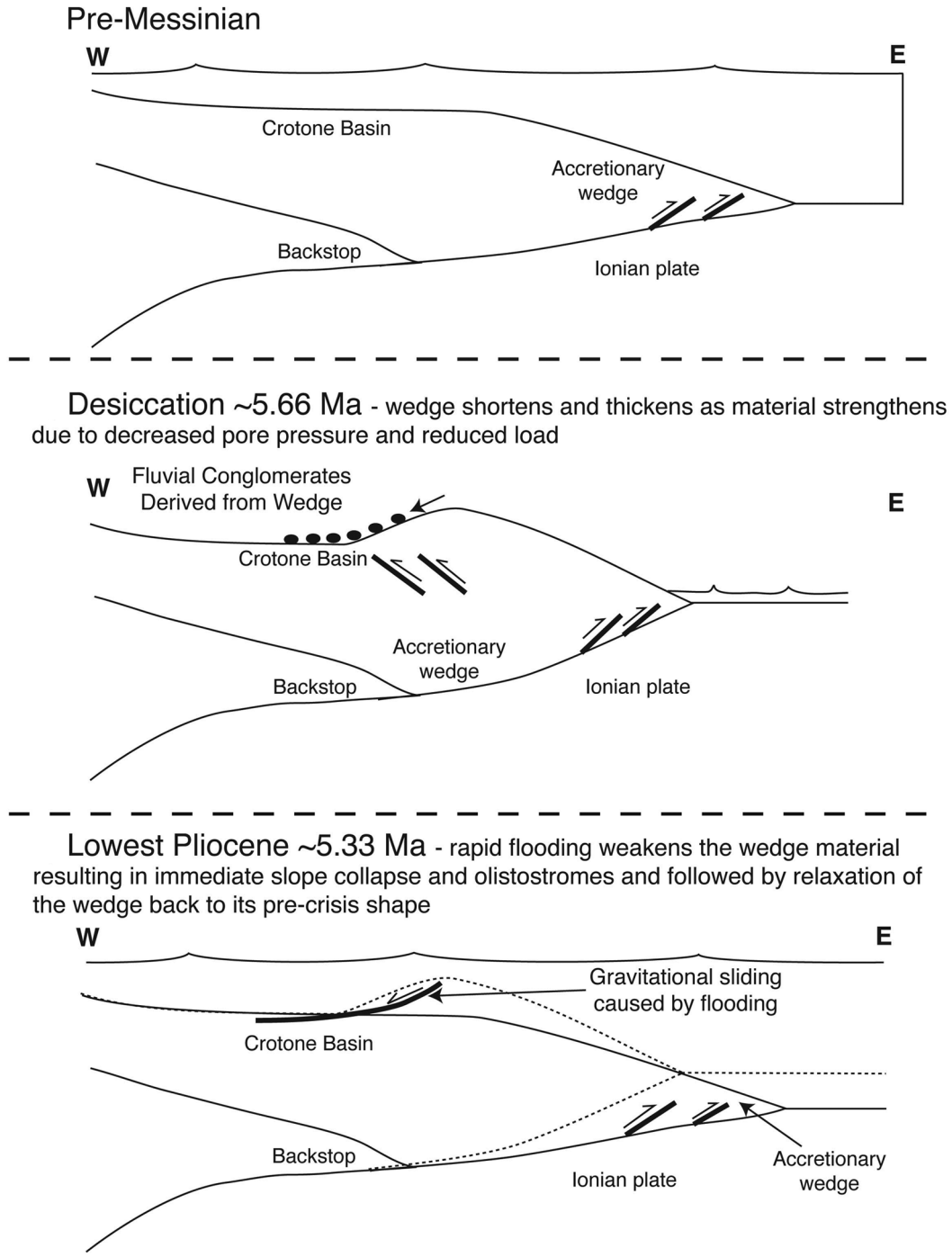

Figure 11. A three-stage conceptual model of accretionary wedge dynamics in response to the Messinian salinity crisis. This model accounts for: isoclinal folds in the accretionary material (Figure 7); westward thrust emplacement of accretionary material and its sedimentary cover up to the Messinian units (Figures 8 and 9); the olistrostrome deposits and possible injections within the Messinian units (Figures 4a and 8); and for the systematic fractures in the Carvane Conglomerate (section 6).

bedding-controlled, topographic low across the study area. The north limb of the Seccata Syncline is composed of south-dipping Messinian units and Pliocene sandstones. Downsection, this structure is coincident with the Messinian ramp. The southern limb of this syncline (northern limb of fold #3) is composed of north-dipping Pliocene and conformable Messinian strata underneath.

[33] Other than the regional ramp shown in Figure 15, faulting of the Messinian units is primarily along bedding or at a very low angle to bedding and is recognized from

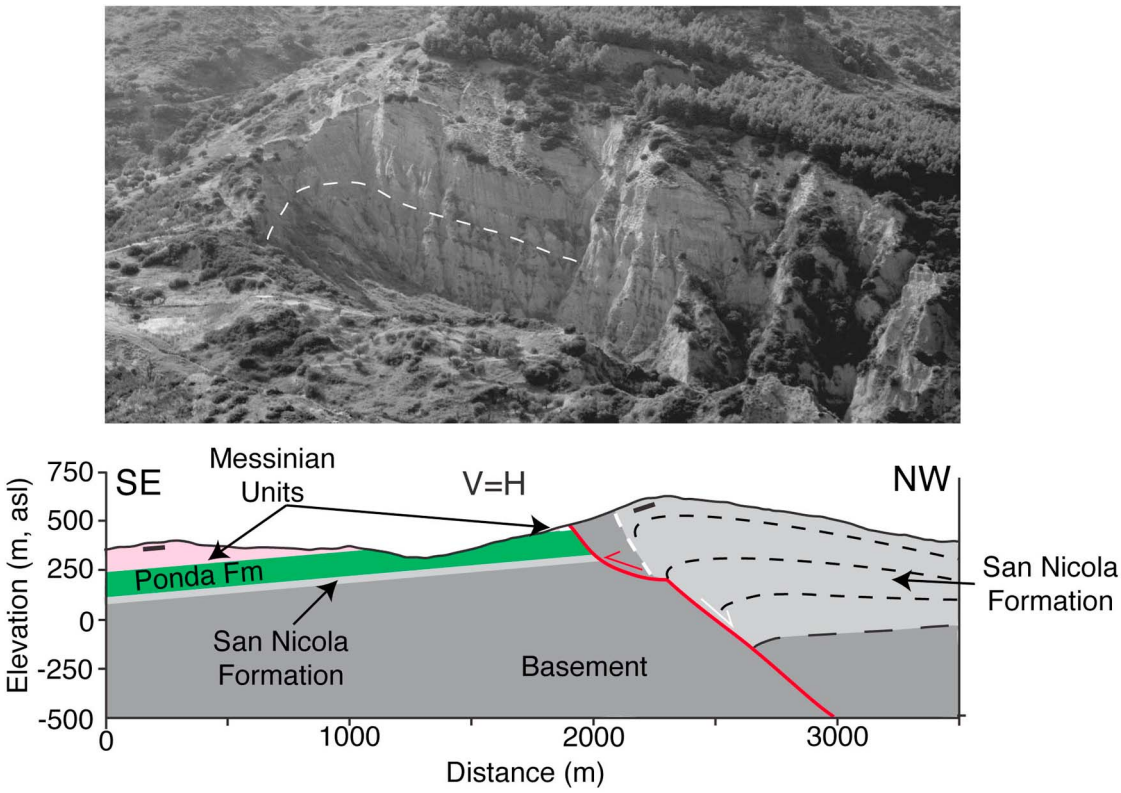

Figure 12. The San Nicola inverted basin at the southern-most exposure of the SNF. The section schematically shows gradual increase in thickness from the Scala Coeli well southward to the SNF and the dramatic decrease in thickness on the footwall side across the fault. This syntectonic sedimentation spans the San Nicola and lower Ponda formations. Messinian units next to the fault shows no evidence of thickness or facies transitions. Thus, the basin-forming extension wanes before the Messinian and thrust reactivation starts afterward.

secondary structures. We ascribe the prevalence of bedding shear to the unusual strength anisotropy: stronger gypsum sandstone layers interbedded with thin, weak gypsum-clay layers. The implied shortening is large. It could be partially absorbed by folding, layer-parallel shortening, and possibly by syntectonic erosion of the hanging wall.

[34] The large scale thrust faults and folds involving the Pliocene and older strata are widely distributed and suggest overall shortening to the north and northwest and can be tested with mesoscale stress and strain indicators in the Messinian and Pliocene units. These structures do not take up much of the slip, but are useful for determining the orientation of shortening and direction of transport. We measured folds, faults, pressure solution fabric (stylolites), extensional joints, drag on foliations, and strain markers in Pliocene and Messinian strata to better define the Pliocene shortening event. In general, the kinematic data from both Messinian and Pliocene structures show a north-south shortening event and a northward vergence (Figure 14).

[35] The southern boundary of the BMPA is defined by a sharp morphological shift, from elevated and folded lower to middle Pliocene sediments to low-lying, middle Pliocene deposits. A late stage normal fault, coincident with the axis of the fold drops the southern limb and prevents observation of fold closure.

6.3. BMPA Interpretation

[36] The asymmetry of folds #1 and #3 of the BMPA (Figure 4) and their relationship with the basal thrust are well exposed in the western part of the study area and are the basis for the interpretation of the BMPA as a composite contractional antiform, rooted by a set of imbricate thrust faults verging north to northwest (sections A, B, C in Figure 4b). As predicted by classical fault-bend-fold geometry, the bedding attitudes on the backlimbs of anticlines are similar to the attitudes of the faults that root the folds. Thus, structures can be traced to the east even where they are not well exposed. The Seccata Syncline and fold #1 bracket the BMPA and show broadening to the west.

[37] The data presented in Figure 14 support the contention that the anticlinorium is a north to northwest verging, contractional structure. Its southern boundary is defined by a late-stage normal fault that follows the axis of fold #1 and may be rooted in the basal thrust fault of the BMPA, essentially reactivating the proposed ramp in extension. In this interpretation, fold #1 is a ramp-flat structure and the BMPA is the fault-bend fold associated with this ramp. The buried ramp is possibly reactivating a Serravallian normal fault and inverting a basin, similar to the SNF. The proposed buried ramp and the ramp exposed in the Messinian units mark the basal thrust fault rising up-section in the direction of

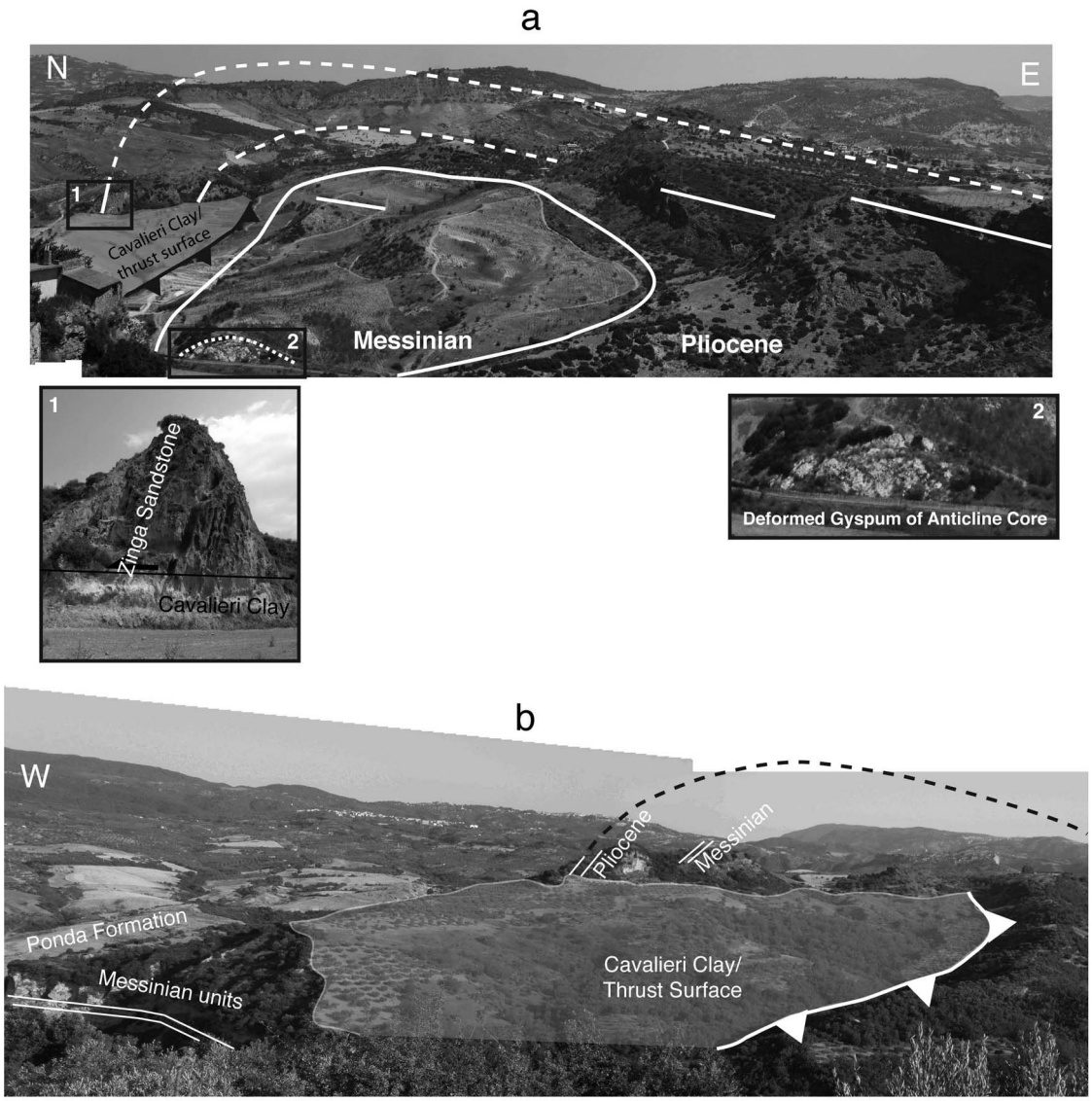

Figure 13. (a) Fold #1 exposes the core of the BMPA along the Neto River. The Pliocene sandstones define an asymmetric anticline with a gently dipping SE limb and a subvertical NW limb (inset 1). Messinian beds are conformable to the Pliocene beds, but become very deformed in the core of the anticline (inset 2). (b) Fold #3, in the far NW of cross-section A, appears at the same structural level as Fold #1, highlighting the consistency of the structure throughout the study area. It is one of the few exposures of older Messinian rocks emplaced on top of younger Pliocene rocks.

vergence. Ramps and imbrications off this main thrust fault fill the flat between the two ramps and are responsible for the series of anticline-syncline pairs that make up the BMPA (Figure 4b, sections A–C).

[38] Many halite diapirs crop out in the Crotone basin, but are confined to the BMPA (Figure 4a). The spatial restriction of the diapirs to the BMPA suggests a genetic relationship. *Zecchin et al.* [2003] suggest that extensional tectonics in the Pliocene resulted in diapirism, which, in turn, created the folds of the BMPA. Although extension cannot be ruled out as a mechanism, we note that halite diapirs occur mostly along the Vitravo and Neto river valleys, suggesting widespread halite under the BMPA that rose in diapirs along minima in vertical load.

[39] The shortening event we document correlates with the middle Pliocene tectonic event recognized in the literature [*Roda*, 1964; *Van Dijk and Okkes*, 1990; *Van Dijk*, 1992; *Van Dijk et al.*, 2000; *Massari et al.*, 2010]. But our results challenge both the direction and duration of shortening that are usually quoted in the literature. Our data point to north-south shortening, which we interpret as a response to arc-parallel shortening as the forearc squeezed through the Apulia-Nubia narrow. *Van Dijk* [1992] and *Massari et al.* [2010] have also recognized N-S shortening structures in the Pliocene, but attributed them to transpression along the SNF and smaller scale strike slip fauts (see Discussion). *Zecchin et al.* [2003, 2004a] concluded the cessation of this shortening occurred the middle Pliocene, prior to deposition

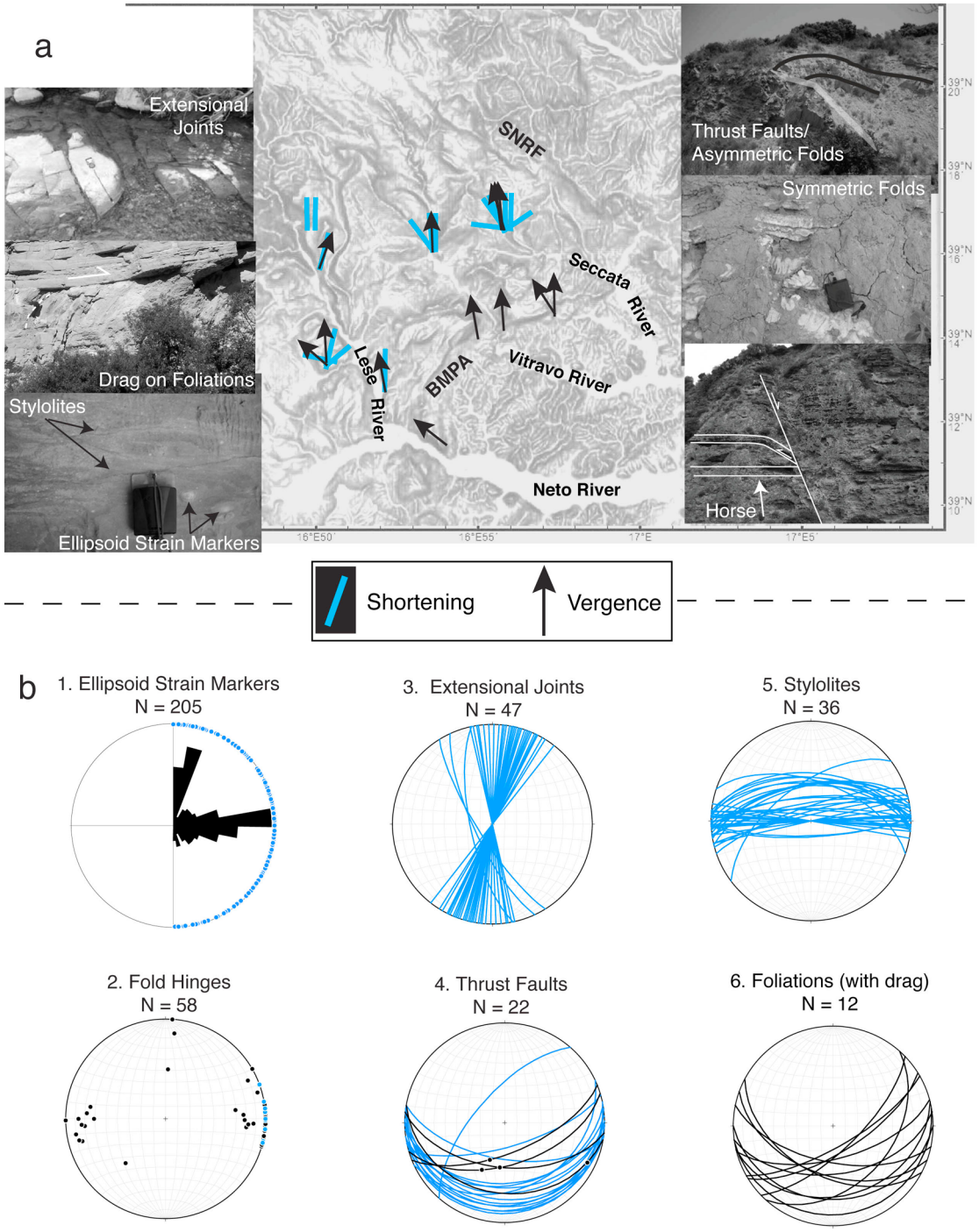

Figure 14. Mesoscale shortening structures in Pliocene and Messinian units. (a) Field examples of structures and a GeoMapApp image of the observation sites, distinguishing between structures that give vergence and those that give shortening. (b) Lower hemisphere, equal area stereonet projections of the kinematic indicators in each class of structures. They are color-coded to show which are shortening structures and which are vergence indicators. Strain ellipsoids are a measurement of the long axis of the nodules and show a wide range of orientations. The black petals show where the orientations cluster since it is unclear just from the data.

of the transgressive Spartizzo Clay. We propose a much longer shortening phase continuing into the late Pleistocene.

[40] The bedding control on faulting makes it difficult to estimate the amount of shortening. Using the estimated thrust front in Figure 4a, 2–3 km of shortening can be ascribed to the ramp and an estimated 1 km absorbed in the BMPA. In order to estimate the contribution of layer parallel shortening, we used the gypsum strain markers (Figure 14a)

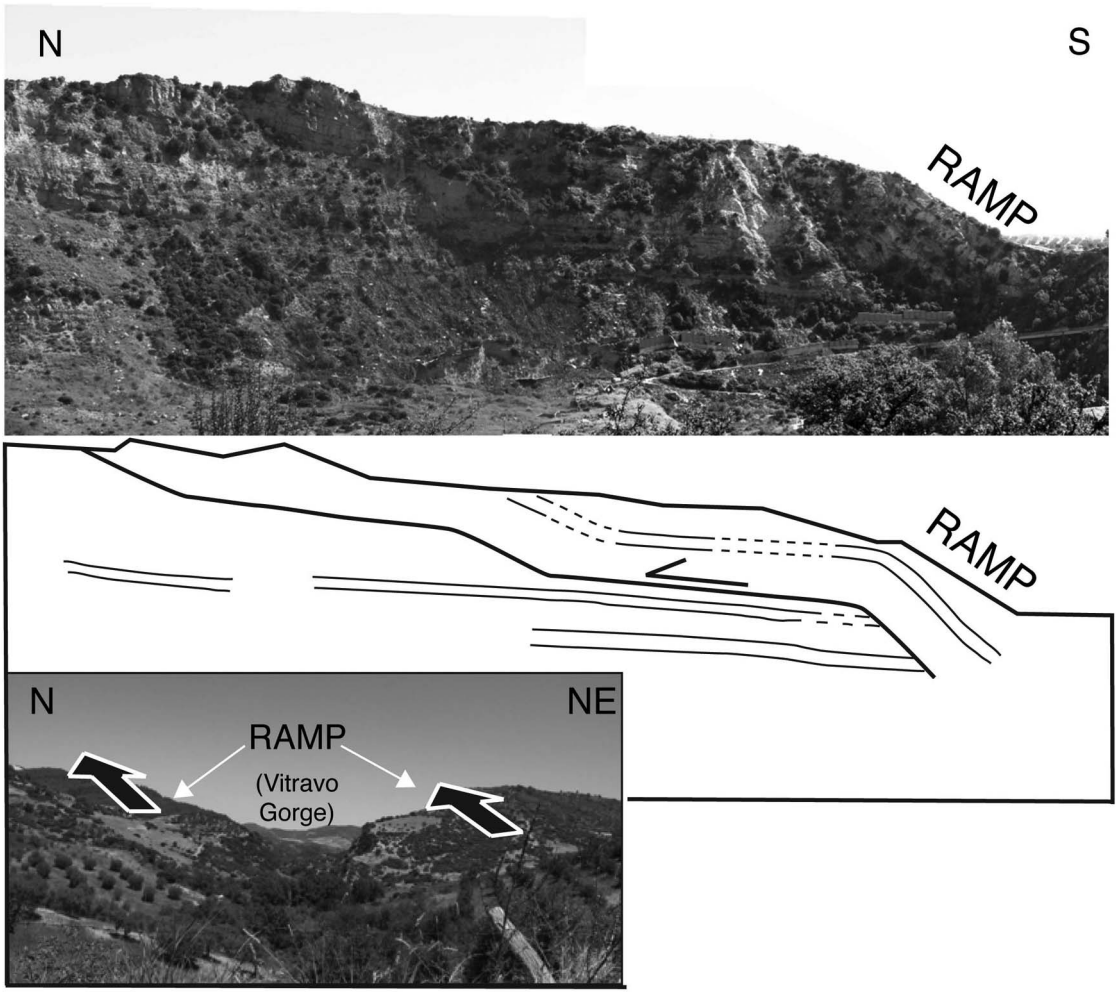

Figure 15. A flat-ramp-flat structure that effectively doubles the Messinian section is clearly exposed along the Lese River (Figure 2b). Line drawing of photo directly below. Inset: a view north along the Vitravo River gorge, cutting through the ramp-controlled morphology of the study area.

as strain indicators, assuming an initial spherical shape. A conservative aspect ratio of 2:1 in the nodules yields an additional 2 km of shortening. We, therefore, roughly estimate 5–6 km of shortening in the Pliocene, excluding the shortening accounted for by the buried ramp and possible imbrication in the core of the BMPA.

7. Discussion

7.1. The Role of Strike-Slip Faulting in the Crotone Basin

[41] Many authors follow *Van Dijk and Okkes* [1991] and *Van Dijk* [1992] in proposing that a pull-apart associated with sinistral faulting oblique to the forearc has controlled subsidence in the Crotone basin [e.g., *Cifelli et al.*, 2007;*Tansi et al.*, 2007]. This idea is in contrast with the interpretation of a constructed forearc basin that does not require a basin-bounding fault and is at odds with our data. The proposed pull-apart coincides with a stepover between the sinistral SNF and Petilia Fault (Figure 1) and is assumed have been active since 12 Ma. Above, however, we showed that the basin related to the SNF was to the north of the SNF, not to the south, as the pull-apart model predicts. Furthermore, the inversion of such a pull-apart basin [*Van Dijk*, 1992] would require a reversal in motion along the SNF, from sinistral to dextral. A major, dominantly trancurrent fault is characterized by local, geometric anomalies causing transpression and transtension and leading to both ridges and basins [e.g., *Mann*, 2007]. In contrast, the entire SNF seems to be affected by two distinct temporal phases: an extensional phase in the Serravallian and a shortening phase in the Pliocene. Tectonics is prominently quiescent in the Crotone basin during the Tortonian, when subduction-rollback is at its fastest. This behavior is inconsistent with an active strike-slip fault bounding the basin, but is consistent with the interpretation of the Crotone basin as a forearc basin, where sediments can accumulate without large-scale, bounding faults [*Dickinson and Seely*, 1979]. The SNF cannot be interpreted as the northern STEP fault of the Calabrian system [*Govers and Wortel*, 2005], since it would only recently have become active and should not show deformation in the Serravallian.

[42] Recent work [*Galli and Scionti*, 2006; *Massari et al.*, 2010; *Speranza et al.*, 2010] documenting strike slip faulting in the Crotone basin must be acknowledged. These works provide compelling arguments for active strike slip faults

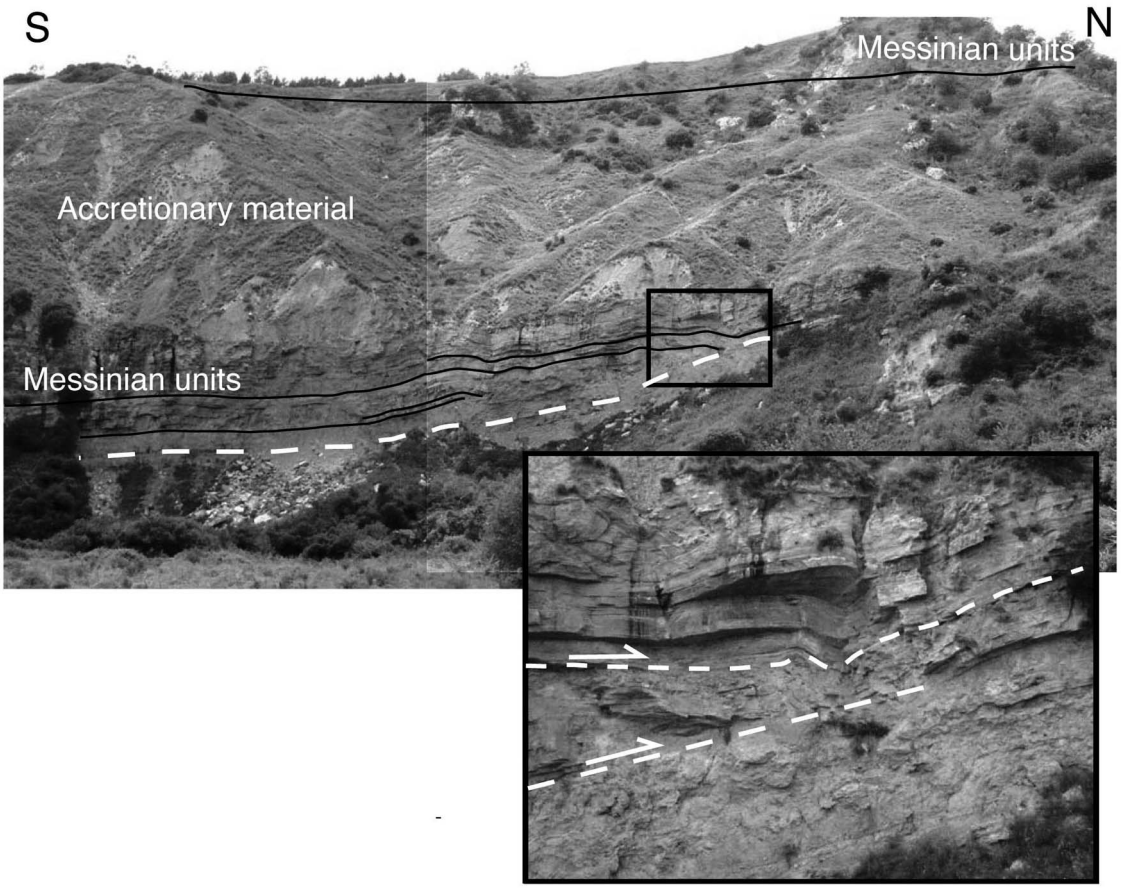

Figure 16. Pervasive bedding parallel shear within the Messinian units is manifested by a subtle, upsection cut by a fault near its tip. This fault and the roof thrust above it delineate a horse updip from the ramp, probably one of many in an imbricate system that accounts for substantial shortening.

south and west of our study area. Our data do not challenge the conclusion that strike slip motion has occurred in this area. But it is not necessary to invoke crustal scale shear zones generating a pull-apart to account for block rotation and strike slip faults. The interpretation of the Crotone basin as a forearc basin, sitting above an active subduction zone can readily account for rotation, differential uplift and subsidence, and minor faults with variable kinematics. We do not challenge transform motion or rotation in the Crotone basin, only that transform faults are responsible for the lateral displacement of the forearc. Instead, our data support evolution of the basin in a classic forearc setting, subsiding throughout rollback as the forearc moved passively and rigidly to the southeast.

7.2. Contraction and Thin-Skinned Extension During the Pliocene

[43] In previous work, the deposition of Pliocene sediments in the Crotone basin was interpreted to occur in an extensional regime, interrupted by a brief contractional event [*Roda*, 1964; *Van Dijk*, 1992; *Zecchin et al.*, 2003, 2004a, 2006]. Instead, we propose that a deep-rooted contractional event occurred throughout the Pliocene with associated surficial extension. The decoupling between tectonic stresses at depth and gravitational stress near the surface can be explained by the extreme weakness to bedding parallel shear of some of the units.

[44] *Zecchin et al.* [2003, 2004a] document growth sedimentation in six, Pliocene-age normal fault bounded half-grabens before and after a brief early Pliocene shortening event. They assume the shortening event is dynamically incompatible with the extensional structures and so postulated two different stress regimes active at different times. Alternatively, we propose that the contraction and the extensional growth structures are contemporaneous and related. The normal growth faulting is highly listric [*Zecchin et al.*, 2004a; *Mellere et al.*, 2005] and underlying Messinian units including the Carvane Congloemrate are not deformed in extension. Thus, we propose a shallow rooted extension that was probably rooted in the weak Cavalieri Clay. Layer-parallel shear in the weak Cavalieri Clay could decouple topographic stress above from the tectonic stress below. In our hypothesis, the structural growth of the anticlinorium provided the topographic stress, while bedding shear in the Cavalieri Clay led to creep-collapse along the flanks of the BMPA. In support of this hypothesis are the following observations: First, the grabens are remarkably parallel to the axis of the anticlinorium and are concentrated along it (Figure 17). Second, nowhere in the our study area did we find evidence of significant normal faulting offsetting the

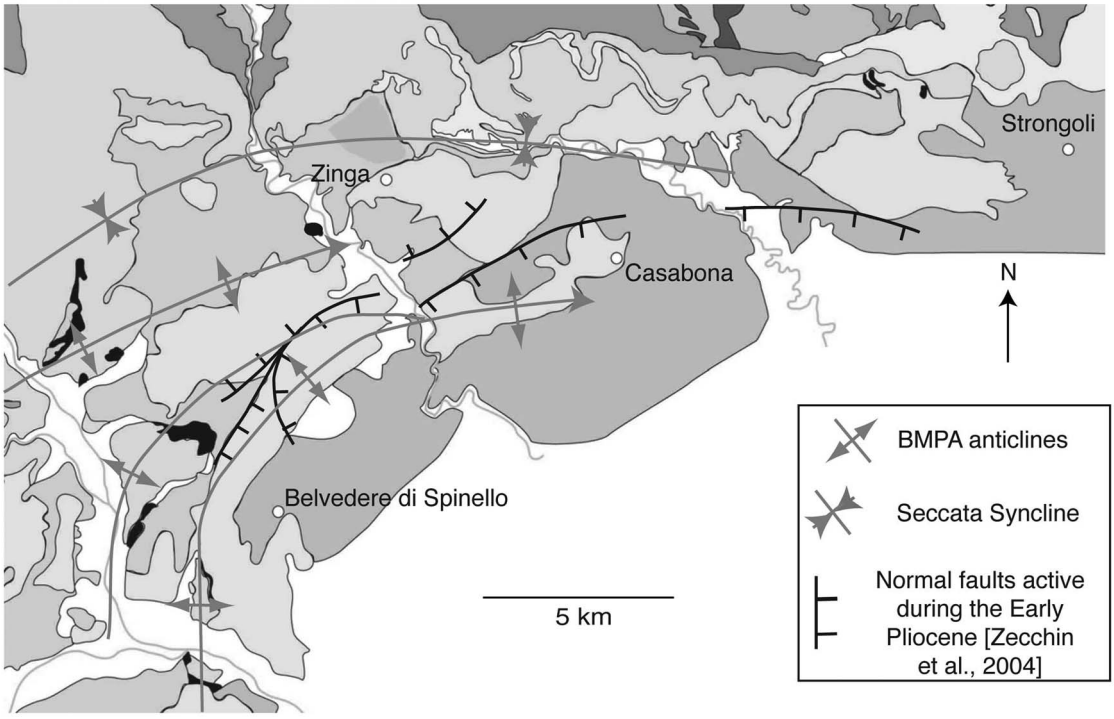

Figure 17. Spatial relationship between the Pliocene shallow rooted faults and half-grabens mapped by *Zecchin et al.* [2004a] and the shortening folds of the BMPA. Extensional structures are concentrated on the structural highs caused by the contraction and folding. This correlation supports the hypothesis that superficial normal faulting and deep-rooted shortening are synchronous. Thus, the late Pliocene extension may signal contraction into the late Pliocene rather than excluding it.

Messinian units, which is generally cliff-forming and is, by far, the best exposed section of the Neogene sequence. Third, normal faulting on top of active compressional folds has been described elsewhere (e.g., thrust top and piggyback basins) [*Ori and Friend*, 1984; *DeCelles and Giles*, 1996] and may be favored in this case because of the mechanical weakness of the clay units below the competent Pliocene sandstones. According to this interpretation, continued growth of thrust-top basins is symptomatic of continued folding. We thus propose that the shortening event continued to the end of Pliocene when the thrust-top basins ceased to be active [*Mellere et al.*, 2005].

7.3. Reactivation of Structures

[45] Reactivation of pre-existing structures is a key aspect of the deformation history in the Crotone basin. Structures related to the SNF and other faults in the Crotone basin marking the onset of Calabrian rollback offer classical examples of basin inversions. In light of those examples, we tentatively propose a basin inversion along the BMPA (fold #1). Another important consequence of fault reactivation is that fault geometry may be quite different from the ideal, determined from the tectonic stress direction. Thus, the scatter in the strike of faults and folds that accommodated the Pliocene shortening in the Crotone basin (SNF and BMPA) may be more relevant to the orientation of pre-existing extensional faults than to spatial complexities in the direction of shortening. Our kinematic data show a fairly consistent pattern of north to northwest shortening, but pertaining mostly to the Messinian and Pliocene rocks. A kinematic analysis of rocks in the SNF zone would test whether this fault was reactivated by the same shortening event that generated the BMPA and Messinian Ramp, as we postulate.

7.4. Pleistocene Tectonic Upheaval

[46] Tectonic upheaval during the Pleistocene affects the Crotone basin in multiple ways, which are generally consistent with the extension and uplift reported throughout Calabria [*Dumas et al.*, 1988; *Westaway*, 1993; *Tortorici et al.*, 1995; *Cucci and Cinti*, 1998; *Zecchin et al.*, 2004b; *Dewez et al.*, 2008]. The most dramatic local phenomenon is the uplift of the Sila Massif. We are investigating this uplift with a variety of techniques [*Reitz et al.*, 2011], but results will be presented elsewhere.

8. Calabrian Evolution From the Viewpoint of the Crotone Basin

[47] Structural analysis of the Crotone basin provides new constraints on the tectonics of the Calabrian forearc that aid the development of geodynamic models for the evolution of the subduction-rollback system as it passed through the Apulia-Nubia narrow. The following tectonic evolution of the Calabrian phase of subduction is derived from previous concepts about Mediterranean tectonics, but also specifically incorporates the structure and stratigraphy of the Crotone basin (Figure 18).

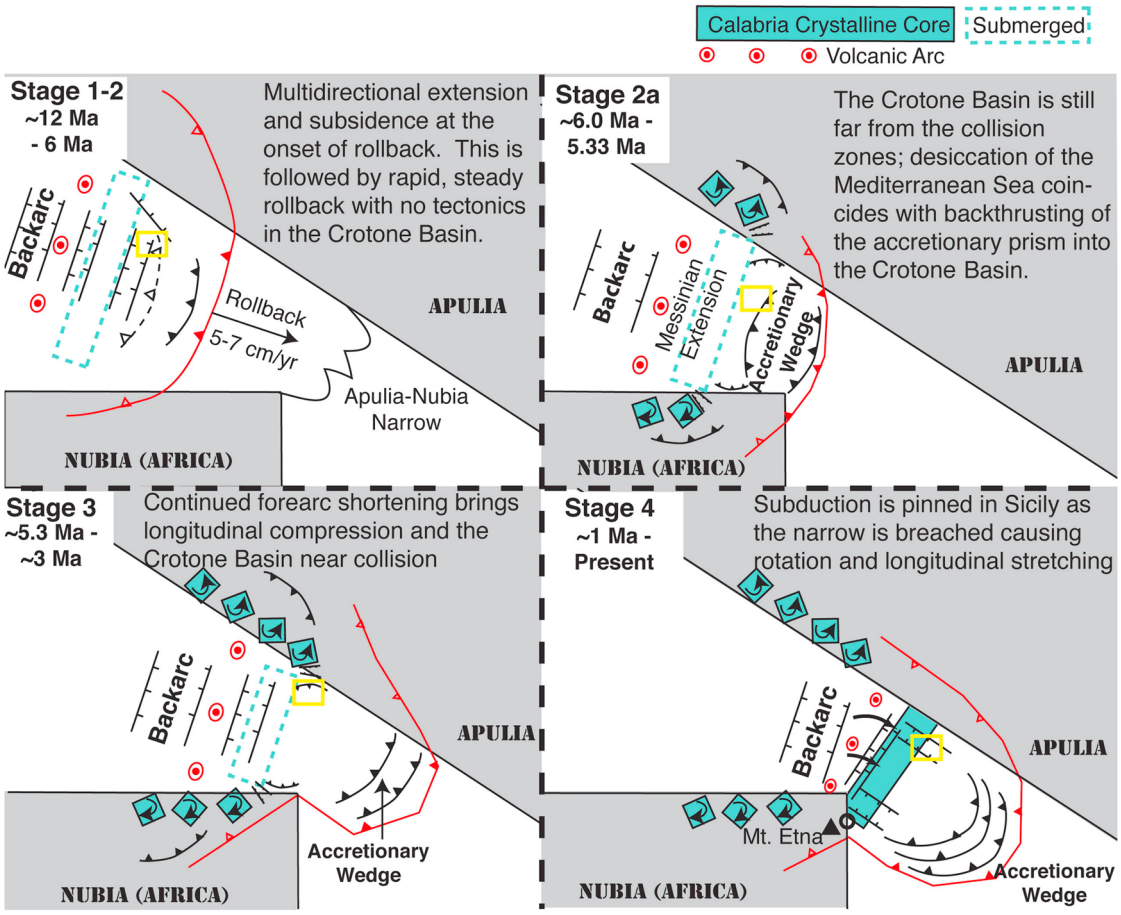

Figure 18. Evolution of the Calabrian Forearc. (top left) Stage 1: Large-scale extension in both backarc and forearc of the system. Most of Calabria was submerged and active accretion was not affecting the Crotone basin at this stage. (top right) Stage 2: Forearc basin extension wanes. Rollback-driven progressive oblique collisions with Apulia and Nubia continued to shorten the forearc, but did not yet affect the Crotone basin. The Messinian salinity crisis destabilized the wedge, which backthrusted onto the Crotone basin. (bottom left) Stage 3: The effects of progressive collision with Apulia were finally recorded in the Crotone basin beginning in the early Pliocene as the arc squeezed through the Apulia-Nubia narrow. This manifested as a N-S shortening in the Crotone basin. (bottom right) Stage 4: The Calabrian Arc has passed through Apulia-Nubia narrow. As the subducting Ionian lithosphere widened, the forearc stretched longitudinally to compensate, leading to boudinage extension, uplift, and rotation of Calabria.

[48] **Stage 1:** Calabria rifted from Corsica and Sardinia in the late Serravallian. Although the Crotone forearc basin was far from the axis of spreading, it experienced extension and subsidence. This initial extension continued through the coarse, coastal sedimentation, but ceased before rapid rollback opened much of the Tyrrhenian basin. The deep-rooted extensional faults persisted as weaknesses in the basement that focused strain during later deformation phases. **Stage 2:** The Crotone basin experienced little tectonism during most of the Calabrian phase of rollback. Collision was occurring at the northern and southern edges of the subduction system (formation of the Apennines and Maghrebides), but these collisions were still far from the Crotone basin. Tectonic quiescence above rapid subduction suggests dynamic equilibrium and a steady state rollback regime. **Stage 2a:** The Messinian salinity crisis drastically altered boundary conditions on the accretionary wedge. Rapid changes in water loads and pore pressure resulted in backthrusting that thickened the wedge and created a structural high abutting the Crotone basin to the east. Gravity flows from this high to the west deposited olistrostromes west into the forearc basin. Subaerial rivers later flowed westward into the basin forming the Carvane Conglomerate. Rapid flooding possibly triggered gravitational slides down the river valleys, which generated the fractures in the Carvane Conglomerate. After the Messinian salinity crisis, the accretionary wedge presumably resumed dynamic conditions similar to before the crisis and the Crotone basin, once again, became isolated from accretion tectonics. **Stage 3:** In the middle Pliocene, the Crotone basin began to experience N-S shortening, parallel to the forearc. Two factors may contribute to this arc-parallel shortening: Progressive collision and tectonic erosion along the outer flanks of the forearc would have brought the Crotone basin close to collision with Apulia in the Pliocene. In this case, the arc-parallel shortening would have been confined to the Crotone basin and adjacent regions.

Alternatively, or in addition, rapid narrowing of the subducting slab forced longitudinal shortening of the forearc as the system squeezed through the Apulia-Nubia narrow. In this case, we expect the arc-parallel shortening to be a regional event that affected the entire Calabrian forearc. **Stage 4:** The mid-Pleistocene uplift may be related to the passive widening of the subducted slab southeast of the narrow. Once through the Apulia-Nubia narrow, widening of the subducted slab requires active, arc-parallel extension of the forearc; essentially the reverse of what we proposed for the Pliocene. This extension is concentrated in the arc-perpendicular basins, forming a boudinage of the forearc. This interpretation also implies that subduction has not ended [*Westaway*, 1993; *Rizzetto et al.*, 2004; *Neri et al.*, 2009], but has passed the chokepoint.

9. Conclusions

[49] 1. Backarc extension and subsidence during reinitiation of subduction-rollback in the Serravallian-Tortonian reached into the forearc as far as the Crotone basin. Faults associated with this extension penetrate basement below the basin and some were later reactivated in contraction.

[50] 2. Tectonic quiescence characterizes the Crotone basin during most of the Calabrian phase of rollback. The forearc rode passively above the retreating megathrust for 6 Myr and 200 km with little to no internal deformation. This suggests a dynamic equilibrium of the subduction-rollback regime and challenges previous interpretations of distinct phases of backarc extension coupled to phases of forearc extension.

[51] 3. In the late Messinian, a structural high developed offshore, east of the Crotone basin and accretionary material was backthrusted onto the outer part of the basin. Olistostomes reached more interior parts of the basin. The direction of emplacement is sub-parallel to systematic fractures in pebbles of the Carvane Conglomerate. The Messinian salinity crisis was likely to induce changes in accretionary wedge dynamics that caused these phenomena.

[52] 4. The Crotone basin experienced a shortening event with N to NW vergence during the Pliocene. The direction of shortening is sub-parallel to the trend of the forearc and is highly oblique to the accretion direction. The passing of the Calabrian forearc through the Apulia-Nubia narrow can account for the arc-parallel shortening in the Pliocene.

[53] 5. Faulting in the Crotone basin is dominated by the basement-rooted normal faults formed at the onset of sedimentation. These faults are later reactivated in contraction. The short pulse of westward backthrusting from the accretionary prism is shallow rooted. These structural phases are consistent with a forearc basin of a subduction system, but is inconsistent with a pull-apart or transtensional basin, as many have proposed for the Crotone basin.

[54] **Acknowledgments.** This manuscript and the ideas presented were improved by field trips and discussions with Thorsten Nagel, Ignazio Guerra, Massimo Zecchin, Claudio Faccenna, Colin Stark, and Michael Steckler. Nicholas Christie-Blick and Michael Steckler helped to greatly improve the manuscript. Rick Allmendinger and Nestor Cardozo for their OSXStereonet Software, which generated all the stereonets in this manuscript. This research was supported by the National Science Foundation grant EAR 06–07687.

References

Amodio Morelli, L., et al. (1976), L'Arco calabro-peloritano nell'orogene appenninico maghrebide, *Mem. Soc. Geol. Ital.*, *17*, 1–60.

Barberi, G., M. T. Cosentino, A. Gervasi, I. Guerra, G. Neri, and B. Orecchio (2004), Crustal seismic tomography in the Calabrian Arc region, south Italy, *Phys. Earth Planet. Inter.*, *147*, 297–314, doi:10.1016/j.pepi.2004.04.005.

Barone, M., R. Dominici, F. Muto, and S. Critelli (2008), Detrital modes in a Late Miocene wedge-top basin, northeastern Calabria, Italy: Compositional record of wedge-top partitioning, *J. Sediment. Res.*, *78*, 693–711, doi:10.2110/jsr.2008.071.

Bonardi, G., W. Cavazza, V. Perrone, and S. Rossi (2001), Calabria-Peloritani Terrane and Northern Ionian Sea, in *Anatomy of an Orogen: The Apennines and Adjacent Mediterranean Basins*, edited by G. B. Vai and I. P. Martini, pp. 287–306, Kluwer Acad., Boston, Mass.

Capraro, L., C. Consolaro, E. Fornaciari, F. Massari, and D. Rio (2006), Chronology of the Middle-Upper Pliocene succession in the Strongoli area: Constraints on the geological evolution of the Crotone basin (southern Italy), *Geol. Soc. Spec. Publ.*, *262*, 323–336.

Cavazza, W., and M. Barone (2010), Large-scale sedimentary recycling of tectonic mélange in a forearc setting: The Ionian basin (Oligocene-Quaternary, southern Italy), *Geol. Soc. Am. Bull.*, *122*(11–12), 1932–1949, doi:10.1130/B30177.1.

Cavazza, W., and P. DeCelles (1998), Upper Messinian siliciclastic rocks in southeastern Calabria (southern Italy): Palaeotectonic and eustatic implications for the evolution of the central Mediterranean region, *Tectonophysics*, *298*, 223–241, doi:10.1016/S0040-1951(98)00186-3.

Cavazza, W., and R. Ingersoll (2005), Detrital modes of the Ionian fore-arc basin fill (Oligocene-Quaternary) reflect the tectonic evolution of the Calabria-Peloritani terrane (southern Italy), *J. Sediment. Res.*, *75*, 268–279, doi:10.2110/jsr.2005.020.

Christie-Blick, N., and K. T. Biddle (1985), Deformation and basin formation along strike-slip faults, *Spec. Publ. Soc. Econ. Paleontol. Mineral.*, *37*, 1–34.

Cifelli, F., M. Mattei, and F. Rossetti (2007), Tectonic evolution of arcuate mountain belts on top of a retreating subduction slab: The example of the Calabrian Arc, *J. Geophys. Res.*, *112*, B09101, doi:10.1029/2006JB004848.

Cucci, L., and F. Cinti (1998), Regional uplift and local tectonic deformation recorded by the Quaternary marine terraces on the Ionian coast of northern Calabria (southern Italy), *Tectonophysics*, *292*, 67–83, doi:10.1016/S0040-1951(98)00061-4.

D'Agostino, N., A. Avallone, D. Cheloni, E. D'Anastasio, S. Mantenuto, and G. Selvaggi (2008), Active tectonics of the Adriatic region from GPS and earthquake slip vectors, *J. Geophys. Res.*, *113*, B12413, doi:10.1029/2008JB005860.

D'Agostino, N., E. D'Anastasio, A. Gervasi, I. Guerra, M. Nedimovic, L. Seeber, and M. Steckler (2011), Forearc extension and slow rollback of the Calabrian Arc from GPS measurements, *Geophys. Res. Lett.*, *38*, L17304, doi:10.1029/2011GL048270.

Davis, D., J. Suppe, and F. A. Dahlen (1983), Mechanics of fold-and-thrust belts and accretionary wedges, *J. Geophys. Res.*, *88*, 1153–1172, doi:10.1029/JB088iB02p01153.

DeCelles, P., and W. Cavazza (1995), Upper Messinian conglomerates in Calabria, southern Italy: Response to orogenic wedge adjustment following Mediterranean sea-level changes, *Geology*, *23*, 775–777, doi:10.1130/0091-7613(1995)023<0775:UMCICS>2.3.CO;2.

DeCelles, P., and K. Giles (1996), Foreland basin systems, *Basin Res.*, *8*, 105–123, doi:10.1046/j.1365-2117.1996.01491.x.

Dewez, T., C. P. Stark, S. Huot, M. Cardinali, M. Lamothe, F. Guzzetti, and L. Seeber (2008), Late Quaternary uplift and coastal landscape evolution in northern Calabria, *Eos Trans. AGU*, *89*(53), Fall Meet. Suppl., Abstract T53B-1930.

Dickinson, W. R., and D. R. Seely (1979), Structure and stratigraphy of forearc regions, *Am. Assoc. Pet. Geol. Bull.*, *63*(1), 2–31.

Dumas, B., P. Gueremy, P. J. Hearty, R. Lhenaff, and J. Raffy (1988), Morphometric analysis and amino acid geochronology of uplifted shorelines in a tectonic region near reggio Calambria, South Italy, *Palaeogeogr. Palaeoclimatol. Palaeoecol.*, *68*, 273–289, doi:10.1016/0031-0182(88)90045-4.

Eidelman, A., and Z. Reches (1992), Fractured pebbles–a new stress indicator, *Geology*, *20*, 307–310, doi:10.1130/0091-7613(1992)020<0307:FPANSI>2.3.CO;2.

Faccenna, C., T. W. Becker, F. Pio Lucente, L. Jolivet, and F. Rossetti (2001), History of subduction and back-arc extension in the Central Mediterranean, *Geophys. J. Int.*, *145*, 809–820, doi:10.1046/j.0956-540x.2001.01435.x.

Faccenna, C., C. Piromallo, A. Crespo-Blanc, L. Jolivet, and F. Rossetti (2004), Lateral slab deformation and the origin of the western Mediterranean arcs, *Tectonics*, *23*, TC1012, doi:10.1029/2002TC001488.

Flecker, R., and R. M. Ellam (2006), Identifying Late Miocene episodes of connection and isolation in the Mediterranean-Paratethyn realm using Sr isotopes, *Sediment. Geol.*, *188–189*, 189–203, doi:10.1016/j.sedgeo.2006.03.005.

Galli, P., and V. Scionti (2006), Two unknown M > 6 historical earthquakes revealed by palaeoseismological and archival researches in eastern Calabria (southern Italy); seismotectonic implications, *Terra Nova*, *18*(1), 44–49, doi:10.1111/j.1365-3121.2005.00658.x.

Ghisetti, F., and L. Vezzani (1981), Contribution of structural analysis to understanding the geodynamic evolution of the Calabrian Arc (southern Italy, *J. Struct. Geol.*, *3*(4), 371–381, doi:10.1016/0191-8141(81)90037-7.

Govers, R., and M. J. R. Wortel (2005), Lithosphere tearing at STEP faults: Response to edges of subduction zones, *Earth Planet. Sci. Lett.*, *236*, 505–523, doi:10.1016/j.epsl.2005.03.022.

Guarnieri, P. (2004), Structural evidence for deformation by block rotation in the context of transpressive tectonics, northwestern Sicily (Italy), *J. Structural Geol.*, *26*(2), 207–219, doi:10.1016/S0191-8141(03)00102-0.

Gueguen, E., C. Doglioni, and M. Fernandez (1998), On the post-25 Ma geodynamic evolution of the western Mediterranean, *Tectonophysics*, *298*(1–3), 259–269, doi:10.1016/S0040-1951(98)00189-9.

Gvirtzman, Z., and A. Nur (2001), Residual topography, lithospheric structure and sunken slabs in the central Mediterranean, *Earth Planet. Sci. Lett.*, *187*, 117–130, doi:10.1016/S0012-821X(01)00272-2.

Jolivet, L., and C. Faccenna (2000), Mediterranean extension and the Africa-Eurasia collision, *Tectonics*, *19*(6), 1095–1106, doi:10.1029/2000TC900018.

Kopp, H., and N. Kukowski (2003), Backstop geometry and accretionary mechanics of the Sunda margin, *Tectonics*, *22*(6), 1072, doi:10.1029/2002TC001420.

Krijgsman, W., F. J. Hilgen, I. Raffi, F. J. Sierro, and D. S. Wilson (1999), Chronology, causes and progression of the Messinian salinity crisis, *Nature*, *400*, 652–655, doi:10.1038/23231.

Malinverno, A., and W. B. F. Ryan (1986), Extension of the Tyrrhenian Sea and shortening in the Apennines as result of a migration driven by sinking lithosphere, *Tectonics*, *5*, 227–245, doi:10.1029/TC005i002p00227.

Mann, P. (2007), Global catalogue, classification, and tectonic origins of restraining- and releasing-bends on active and ancient strike-slip fault systems, *Geol. Soc. Spec. Publ.*, *290*, 13–142.

Massari, F., G. Prosser, L. Capraro, E. Fornaciari, and C. Consolaro (2010), A revision of the stratigraphy and geology of the south-western part of the Crotone basin (south Italy), *Boll. Soc. Geol. Ital.*, *129*(3), 353–384.

Mattei, M., P. Cipollari, D. Cosentino, A. Argentieri, F. Rossetti, F. Speranza, and L. Di Bella (2002), The Miocene tectono-sedimentary evolution of the southern Tyrrhenian Sea: Stratigraphy, structural, and palaeomangetic data from the on-shore Amantea basin (Calabrian Arc, Italy), *Basin Res.*, *14*(2), 147–168, doi:10.1046/j.1365-2117.2002.00173.x.

McClusky, S., and R. E. Relinger (2010), Arabia/Africa/Eurasia kinematics and the dynamics of Post-Oligocene Mediterranean tectonics, Abstract T14D-01 presented at 2010 Fall Meeting, AGU, San Francisco, Calif. 13–17 Dec.

Mellere, D., M. Zecchin, and C. Perale (2005), Stratigraphy and sedimentology of fault-controlled backstepping shorefaces, Middle Pliocene of Crotone basin, southern Italy, *Sediment. Geol.*, *176*, 281–303, doi:10.1016/j.sedgeo.2005.01.010.

Minelli, L., and C. Faccenna (2010), Evolution of the Calabrian accretionary wedge (central Mediterranean), *Tectonics*, *29*, TC4004, doi:10.1029/2009TC002562.

Moretti, A. (1993), Note sull-evoluzione tettono-stratigrafica del bacino crotonese dopo la fine del Miocene, *Boll. Soc. Geol. Ital.*, *112*, 845–867.

Muttoni, G., L. Lanci, A. Argani, A. M. Hirt, U. Cibin, N. Abrahamsen, and W. Lowrie (2000), Paleomagnetic evidence for a Neogene two-phase counterclockwise tectonic rotation in the Northern Apennines (Italy), *Tectonophysics*, *326*, 241–253, doi:10.1016/S0040-1951(00)00140-2.

Neri, G., B. Orecchio, C. Totaro, G. Falcone, and S. Presti (2009), Subduction beneath southern Italy close the ending: Results from seismic tomography, *Seismol. Res. Lett.*, *80*(1), 63–70.

Nicolosi, I., F. Speranza, and M. Chiappini (2006), Ultrafast oceanic spreading of the Marsili basin, southern Tyrrhenian Sea: Evidence from magnetic anomaly analysis, *Geology*, *34*(9), 717–720, doi:10.1130/G22555.1.

Ogniben, L. (1955), Le argille scagliose del Crotonese, *Mem. Note Inst. Geol. Appl. Napoli*, *6*, 1–72.

Ogniben, L. (1962), Le argille scagliose e I sedimenti messiniani a sinistra del Trionto (Rossano, Cosenza), *Geol. Rom.*, *1*, 255–282.

Ori, G. G., and P. F. Friend (1984), Sedimentary basins formed and carried piggyback on active thrust sheets, *Geology*, *12*, 475–478, doi:10.1130/0091-7613(1984)12<475:SBFACP>2.0.CO;2.

Patacca, E., R. Sartori, and P. Scandone (1990), Tyrrhenian basin and Apenninic arcs: Kinematic relation since late Tortonian times, *Mem. Soc. Geol. Ital.*, *45*, 425–451.

Reitz, M., L. Seeber, J. Schaefer, and M. Steckler (2011), Using relict landscapes and cosmogenic ^{10}Be to constrain spatial and temporal variations in uplift, Calabria, southern Italy, Abstract EP43C-0702 presented at 2011 Fall Meeting, AGU, San Francisco, Calif. 5–9 Dec.

Rizzetto, C., A. Marotta, and R. Sabadini (2004), The role of trench retreat on the geometry and stress regime in the subduction complexes of the Mediterranean, *Geophys. Res. Lett.*, *31*, L11604, doi:10.1029/2004GL019889.

Roda, C. (1964), Distribuzione e facies dei sedimenti neogenici nel bacino Crotonese, *Geol. Rom.*, *3*, 319–366.

Roda, C. (1967), I sedimenti neogenici autoctoni ed alloctoni della zona di Ciro-Cariati (Catanzaro e Cosenza), *Mem. Soc. Geol. Ital.*, *6*, 137–149.

Rosenbaum, G., and G. S. Lister (2004), Neogene and Quaternary rollback evolution of the Tyrrhenian Sea, the Apennines, and the Sicilian Maghrebides, *Tectonics*, *23*, TC1013, doi:10.1029/2003TC001518.

Rosenbaum, G., G. S. Lister, and C. Duboz (2002), Reconstruction of the tectonic evolution of the western Mediterranean since the Oligocene, *J. Virtual Explor.*, *8*, 107–126, doi:10.3809/jvirtex.2002.00053.

Roveri, M., A. Bernasconi, M. E. Rossi, and C. Visentin (1992), Sedimentary evolution of the Luna field area, Calabria, southern Italy, in *Generation, Accumulation, and Production of Europe's Hydrocarbons II, Spec. Publ. Eur. Assoc. Pet. Geosci.*, vol. 2, pp. 217–224, Springer, Berlin.

Ryan, W. B. F. (2009), Decoding the Mediterranean salinity crisis, *Sedimentology*, *56*, 95–136, doi:10.1111/j.1365-3091.2008.01031.x.

Speranza, F., P. Macrì, D. Rio, E. Fornaciari, and C. Consolaro (2010), Paleomagnetic evidence for a post–1.2 Ma disruption of the Calabria terrane: Consequences of slab breakoff on orogenic wedge tectonics, *Geol. Soc. Am. Bull.*, *123*(5–6), 925–933.

Tansi, C., F. Muto, S. Critelli, and G. Iovine (2007), Neogene-Quaternary strike-slip tectonics in the central Calabrian Arc (southern Italy), *J. Geodyn.*, *43*, 393–414, doi:10.1016/j.jog.2006.10.006.

Tortorici, L., C. Monaco, C. Tansi, and O. Cocina (1995), Recent and active tectonics in the Calabrian Arc (southern Italy), *Tectonophysics*, *243*, 37–55, doi:10.1016/0040-1951(94)00190-K.

Vai, G. B., and I. P. Martini (Eds.) (2001), *Anatomy of an Orogen: The Apennines and Adjacent Mediterranean Basins*, Kluwer Acad., Boston, Mass.

Van Dijk, J. P. (1992), Late Neogene fore-arc basin evolution in the Calabrian Arc (central Mediterranean): Tectonic sequence stratigraphy and dynamic geohistory, PhD thesis, Univ. of Utrecht, Utrecht, Netherlands.

Van Dijk, J. P., and M. Okkes (1990), The analysis of shear zones in Calabria; implications for the geodynamics of the central Mediterranean, *Rev. Ital. Paleontol. Stratigr.*, *96*, 241–270.

Van Dijk, J. P., and M. Okkes (1991), Neogene tectonostratigraphy and kinematics of Calabrian basins; Implications for the geodynamics of the central Mediterranean, *Tectonophysics*, *196*, 23–60, doi:10.1016/0040-1951(91)90288-4.

Van Dijk, J. P., et al. (2000), A regional structural model for the northern sector of the Calabrian Arc (southern Italy), *Tectonophysics*, *324*, 267–320, doi:10.1016/S0040-1951(00)00139-6.

Westaway, R. (1993), Quaternary uplift of southern Italy, *J. Geophys. Res.*, *98*, 21,741–21,772, doi:10.1029/93JB01566.

Zecchin, M., F. Massari, D. Mellere, and G. Prosser (2003), Architectural styles of prograding wedges in a tectonically active setting, Crotone basin, Southern Italy, *J. Geol. Soc.*, *160*, 863–880, doi:10.1144/0016-764902-099.

Zecchin, M., F. Massari, D. Mellere, and G. Prosser (2004a), Anatomy and evolution of a Mediterranean-type fault bounded basin: The lower Pliocene of the northern Crotone basin (southern Italy), *Basin Res.*, *16*, 117–143, doi:10.1111/j.1365-2117.2004.00225.x.

Zecchin, M., R. Nalin, and C. Roda (2004b), Raised Pleistocene marine terraces of the Crotone peninsula (Calabria, southern Italy): Facies analysis and organization of their deposits, *Sediment. Geol.*, *172*, 165–185, doi:10.1016/j.sedgeo.2004.08.003.

Zecchin, M., D. Mellere, and C. Roda (2006), Sequence stratigraphy and architectural variability in growth fault-bounded basin fills: A review of Plio-Pleistocene stratal units of the Crotone basin, southern Italy, *J. Geol. Soc.*, *163*, 471–486, doi:10.1144/0016-764905-058.